JOURNAL OF NEUROPHYSIOLOGY
Vol. 73, No. 1, January 1995. *Printed in U.S.A.*

Short- and Long-Range Neuronal Synchronization of the Slow (<1 Hz) Cortical Oscillation

F. AMZICA AND M. STERIADE
Laboratoire de Neurophysiologie, Faculté de Médecine, Université Laval, Quebec G1K 7P4, Canada

SUMMARY AND CONCLUSIONS

1. Multisite, extra- and intracellular recordings were carried out in cats under ketamine and xylazine anesthesia to assess the degree of synchrony and time relations among cellular activities in various neocortical fields during a slow (<1 Hz) oscillation consisting of long-lasting depolarizing and hyperpolarizing phases.

2. Recordings were performed from visual areas 17, 18, 19, and 21, association suprasylvian areas 5 and 7, motor pericruciate areas 4 and 6, as well as some related thalamic territories, such as the lateral geniculate (LG), perigeniculate (PG), and rostral intralaminar nuclei. We used spike analyses (auto- and cross-correlograms) to reveal rhythmicities, time relations and coherence properties, analyses of field potentials recorded through the same microelectrodes as used for unit discharges (auto-and cross-correlation functions and their spectral equivalents), and spike-triggered averages. The results are based on 194 groups of neurons with a total of 591 neurons. Seventeen groups included intracellular recordings of cortical neurons with membrane potentials more negative than −60 mV and overshooting action potentials.

3. The most obvious and frequent signs of neuronal synchrony were found within and between association areas 5 and 7 and 18/19 and 21. Closely located cells or neuronal pools were also "closer" in time. The shortest mean time lag was found between cells within adjacent foci (1–2 mm) of areas 5 and 7 and was 12 ± 11.2 (SE) ms, with more caudal neurons preceding the rostral ones in 70% of cases. In visual cortical fields, the time lag between areas 18/19 and 21 neurons was 27.6 ± 36 ms, between areas 17 and 21 was 36.2 ± 47.8 ms, and between areas 18/19 and 17 was 40 ± 73 ms. In the majority of cases, neuronal firing in area 21 preceded that in areas 18/19. The longest time lags were found in distant recordings from visual and motor areas, with a mean of 124 ± 86.8 ms, although in some cell groups the time intervals between neuronal firing in areas 18/19 or 21 and areas 4 or 6 were as short as ~20 ms.

4. Similar time relations were found in those instances in which the unit firing of the same cortical neuron was used as reference in spike triggered averages and was related to the field potential recorded from an adjacent area before impaling a neuron and, thereafter, to membrane potential fluctuations after impaling the cell.

5. The PG reticular thalamic neurons reflected the slow cortical oscillation in 75% of multisite recordings. The coherence between the slow rhythm of visual cortical cells and LG thalamocortical neurons was observed in 58% of cases. One-third of LG neurons displayed the intrinsically generated, clocklike delta oscillation that occurred synchronously in simultaneously recorded LG cells.

6. We discuss several possible scenarios implicated in the genesis of the slow cortical oscillation. Although relatively short time lags may be ascribed to direct and oligo- or multisynaptic connections between adjacent or distantly located cortical areas, long time lags (>50 ms) presumably involve inhibition-rebound sequences within the cortex or corticothalamocortical loops. In view of recent data indicating that the blockage of the slow oscillation during activated states could be achieved through a selective suppression of long-lasting inhibitory phases, we suggest that the major factors underlying short- or long-range neuronal synchrony during the slow oscillation are prolonged hyperpolarizations in cortical neuronal assemblies.

INTRODUCTION

Recently, we described a slow (<1 Hz) oscillation of intracellularly recorded neocortical and thalamic neurons and proposed that this oscillation is the emergent activity of a synchronized network (Steriade et al. 1993b,c,d). The concepts of synchrony and of an antinomy between synchronized and desynchronized electroencephalographic (EEG) patterns were widely used over the past six decades to distinguish the high-amplitude slow waves during sleep from the low-amplitude fast waves during wakefulness. Probably the first to suggest that the amplitude of EEG waves is related to the degree of neuronal synchrony were Adrian and Matthews (1934). However, when inferring the process of synchrony among neurons, one has to rely on simultaneous recordings from multiple sites.

Most studies on cortical synchrony dealt with information processing in the visual (see Singer 1993, for a review), auditory (Dickson and Gerstein 1974; Frostig et al. 1983), and sensorimotor (Murthy and Fetz 1992; Smith and Fetz 1989) cortices. The spontaneous activity of cortical neurons during different behavioral states was less often subject to correlation analysis (but see Noda and Adey 1970).

The present paper demonstrates, on the basis of multisite, extra- and intracellular recordings from neocortical suprasylvian associational areas 5 and 7, pericruciate motor areas 4 and 6, and visual areas 17, 18, 19, and 21, that the slow (<1 Hz) oscillation is the emergent activity of a synchronized cortical network. Some of these results have been presented in abstract form (Amzica and Steriade 1993).

METHODS

Animal preparation

The experiments were conducted on 28 cats under ketamine (10–15 mg/kg) and xylazine (2–2.5 mg/kg) anesthesia. Additional doses of anesthetic were injected at the first sign of diminished amplitude and increased frequency of the EEG, to maintain a constant pattern of synchronized EEG throughout the experiment. To further eliminate painful stimuli, all incised and pressure points were infiltrated with lidocaine. All animals were paralyzed with gallamine triethiodide and artificially ventilated with control of the end-tidal CO_2 concentration at 3.7 ± 0.2% (mean ± SE). Rectal

temperature (37–38°C) and heartbeat were continuously monitored. The stability of recordings was ensured by bilateral pneumothorax, cisternal drainage, hip suspension, and by filling the hole made in the calvarium with 4% agar dissolved in saline.

The gross electrical brain activity (EEG) was recorded through stainless steel screws placed into the bone in the vicinity of the single-cell recording site or contralaterally. Coaxial electrodes were inserted closely to the site of cellular recording, with the ring at the cortical surface and the tip at a depth of ~0.6 mm (ECoG). Besides, electrothalamogram (EThG) was recorded through the coaxial electrodes inserted in appropriate thalamic nuclei.

At the end of the experiments, the animals were deeply anesthetized with a lethal dose of pentobarbital sodium (55 mg/kg).

Recording

Intracellular recordings were done with glass micropipettes filled with a 3-M solution of K acetate (impedance: 25–35 MΩ), whereas extracellular recordings were performed with coarser pipettes (5–10 MΩ) and/or with tungsten microelectrodes (impedance: 1–10 MΩ). The electrodes were held and manipulated by three microdrivers. Up to four distinct electrodes, at 1.5-mm distance, were mounted on one microdrive. This technique enabled simultaneous recording from up to six distinct sites. A high-impedance amplifier with active bridge circuitry was used for intracellular recording and current injection. Other a.c. amplifiers were used for extracellular recordings. All channels were digitally recorded on tape (bandpass d.c. to 9 kHz) and fed to a computer for off-line analysis at a sampling rate of 20 kHz.

Data processing

We focused on spike analyses to disclose firing properties (interspike interval histograms), rhythmicities and their strength (autocorrelograms), and time relations together with coherence properties (cross-correlograms). The principles of spike analyses are described elsewhere (Aertsen and Gerstein 1985; Gerstein et al. 1978; Moore et al. 1966). Extracellular recordings were low-pass filtered at 100 Hz to prevent triggering from false events due to ample slow waves. Because the membrane potential (V_m) of cortical neurons recorded in vivo is around −70 mV (Nuñez et al. 1993; Steriade et al. 1993c), the action potentials are not faithful translators of membrane excitatory-inhibitory slow oscillations. Central peaks around zero time lag in cross-correlograms may result from either common excitation or common inhibition (Fetz et al. 1991; Krüger 1983; Singer 1993). Besides, a cross-correlogram results from an averaging procedure, and this might mask a dynamic shift in temporal relation between two units (Steriade and Amzica 1994).

Thus, because of the relative lack of precision of spike analyses, we complemented the data processing by analyses of focal (field) potentials and/or cortical EEG waves treated as time series. The focal waves were obtained by filtering the extracellular recording between d.c. and 30 Hz. The occurrence of action potentials during depth-negative field potentials and of silent neuronal activity during depth-positive cortical waves (Contreras and Steriade 1995) was taken as a condition for the focal waves to faithfully reflect membrane potential variations of surrounding cell populations. Autocorrelation, cross-correlation functions, and their spectral equivalents (fast Fourier transforms, FFTs) were computed according to the mathematical relations described by Bendat and Piersol (1980). In this paper auto- and cross-correlograms will refer to spike analysis, whereas auto- and cross-correlations will refer to field potential analyses.

The largest peak of an FFT or the count of cycles in an autocorrelation yielded the main frequency of the oscillation. Afterward, the strength of the oscillation was assessed by the following procedure: secondary peaks in autocorrelations were counted, and a mark ranging from 0 to 4 was given. If no secondary peak followed the central one, the cell was termed arrhythmic and received 0. If at least four clear peaks followed the central one, the activity was considered as highly rhythmic and marked with 4. For this and intermediate weightings, the envelope of the decaying peaks was also analyzed to determine whether the oscillation was that of a sine wave (mark = 4), of a wideband random noise (mark = 1), or of intermediate values.

Cross-correlation strength was measured on the same scale (0–4) but as a function of the amplitude of the central peak. This was especially easy for wave analyses because of the autoscaling property of cross-correlations (all correlations between 2 waves range between −1 and +1, regardless of the amplitudes of the respective waves). A supplementary scaling procedure was necessary for spike analyses. A "flat" cross-correlation got mark 0, a central peak <0.25 got 1, between 0.25 and 0.5 the mark was 2, from 0.5 to 0.75 it was 3, and >0.75 the mark was 4.

The meaning of the central peak of a cross-correlation is that of a maximum likelihood between the two waves. This is why the time lag between two waves was taken at the abscissa of the maximum of the central peak. Correlation analyses were done on long enough time periods (at least 20 times the slowest time period detectable after d.c. elimination, i.e., minimum 60 s of data was acquired).

Whenever at least one of the neurons recorded simultaneously was rhythmic, we performed spike-triggered averages (STA), i.e., we detected the first spike from the discharge sequence that begins an oscillatory cycle, and we extracted (synchronized on that spike) equal sweeps of field potentials, EEG waves, or intracellular waves recorded simultaneously from other neurons. The averaged sweeps produced the STA, which provided the statistical evidence for interactions between the discharge in the reference neuron and the membrane potential variations of the target cell.

RESULTS

Data base

Our results are based on 194 groups of neurons with a total of 591 cells (in average, 3 cells/group, range 2–8/group). Of these, 66 groups (213 cells) were recorded at short distances (1–2 mm between neighboring electrodes) within areas 5 and 7 of the suprasylvian gyrus, 60 groups (151 cells) were recorded in different visual areas (17, 18, 19, and 21), 41 groups (137 cells) were recorded at distant sites (pericruciate areas 4 and 6, areas 5 and 7, and visual areas 18 and 21), and 27 groups (90 cells) consisted of simultaneously recorded cortical neurons from previously mentioned areas and reticular thalamic or thalamocortical neurons from related thalamic nuclei. Seventeen groups included an intracellular recording with V_m more negative than −60 mV and overshooting action potentials. The definition of cortical areas was based on cytoarchitectural studies of cat neocortex (Gurewitsch and Chatschaturian 1928; Hassler and Muhs-Clement 1964).

General oscillatory properties

The oscillatory features of the spontaneous activity were evaluated according to spike discharges and focal (field) potentials. The majority of cortical neurons (73%) were rhythmic (marks 1–4) in the frequency range (<1 Hz) of the slow oscillation (Steriade et al. 1993c). Oscillations in the delta range (1–4 Hz) were present in 8% of the recorded

TABLE 1. *Oscillatory properties*

Recording site	*n*	Frequency Repartition, %					
		Slow (<1 Hz)		Delta (1–4 Hz)		Arhythmic	
		S	F	S	F	S	F
Areas 5 and 7	169	76	97	6	1.2	18	1.8
Areas 4 and 6	30	67	73	15	17	18	10
Areas 17, 18, 19, and 21	142	71	88	10	5	19	7
Reticular thalamus	31	75	89	10	6	15	5
Dorsal thalamus	25	57	59	33	34	10	7

n is number of cells. S, spikes; F, field.

cells, whereas the remaining 19% of cells were arhythmic (mark 0). Cortical neurons, even when oscillating in the delta frequency range, showed generally an irregular oscillation, often modulated by the slow (<1 Hz) oscillation, and therefore the delta range is poorly represented in spectral analyses or it is overwhelmed by the lower spectrum.

The mean frequency of the oscillation in a representative population of 341 cortical cells was 0.75 ± 0.63 Hz for spike analysis and 0.81 ± 0.46 Hz for field analysis. Table 1 depicts the repartition of the oscillatory activities at different sites according to frequency bands. It appears that, in the slow band, more sites could be declared oscillatory according to their field than to their spike discharge, as would be expected from the rather whimsical discharge pattern during the depolarizing phase of the slow oscillation (see also below). The delta oscillation was present in fewer cortical cells, and it was less frequently disclosed by wave analysis. It was, however, present in ~33% of thalamocortical neurons. The arrhythmic cells displayed slow oscillatory activity during transient epochs but did not meet the above-mentioned criteria of rhythmicity (see METHODS). The mean ± SE marks for slowly oscillating cortical neurons were 2.2 ± 0.9 for spike analysis and 2.8 ± 1.1 for field analysis. This indicates that the synchronous feature of the slow oscillation is better reflected in the focal waves.

Synchrony was not necessarily associated with oscillation, but oscillating cells were more likely to be synchronized than nonoscillating ones. From our sample of 194 groups of multisite recordings, in 54 groups (28%) all cells were very rhythmic (oscillatory mark 4), in 99 groups (51%) the oscillatory mark ranged from 1 to 3, and in the remaining 41 groups (21%) most of the cells were arrhythmic. The 1st category of recordings had a mean correlation mark, as described in METHODS, of 3.35 ± 0.75, the 2nd category had 2.18 ± 1.33, whereas the 3rd had 0.85 ± 1.1. This result suggests that higher states of synchrony are achieved during oscillatory periods.

Synchrony in closely located cells (areas 5 and 7)

The transition from a short EEG-desynchronized epoch toward a synchronized EEG state, associated with changing patterns of neural discharges recorded from areas 5a and 5b, is displayed in Fig. 1. One impaled neuron and the adjacent focal waves in area 5a were recorded together with extracellular discharges and focal waves from area 5b. During the initial period, when field potentials had low amplitudes, the cells were silent or discharged randomly. As soon as the focal waves became more ample and slower, clear spike trains separated by periods of silenced firing occurred in the respective channels. The onset of the depolarizing phase of the oscillation seen in the intracellular trace corresponded to sharp depth-negative focal waves. The hyperpolarized phase of the oscillation coincided with depth-positive field potentials.

To assess synchronization, Fig. 2 displays auto- and cross-correlograms from the spontaneous activity of five neurons, simultaneously recorded with four microelectrodes in the suprasylvian gyrus at the sites indicated in the brain figurine. The distance between neighboring electrodes was 1.5 mm. The five autocorrelograms show that even if the degree of rhythmicity varied from one neuron to the other, all cells displayed oscillations within the same frequency range (0.7–0.8 Hz). In the *bottom row of histograms,* 4 out of the 10 possible cross-correlograms between the neurons are depicted. All show central peaks. In some cases (e.g., cross-correlogram between *cells 2* and *4b*) it was possible to disclose a time precession between the two neurons (see expanded histogram). In the case of neurons discharging single spikes, a main peak with an equal distribution around the zero line was interpreted as due to a common excitatory input (Engel et al. 1992; Fetz et al. 1991). The spectral relation between the oscillations of the five neurons is also contained in the cross-correlograms. Symmetrical secondary peaks at ~1.3 s reflect a coherent oscillation at 0.75 Hz.

Time relations are, however, hardly revealed by cross-correlograms between spikes, mainly because of variability of spike occurrence during the depolarizing phase of the slow oscillation (see intracellular trace in Fig. 1). Besides, the latency of a central peak in a cross-correlogram depends on the binwidth. Figure 1 also showed that there is a close relation between the onset of the depolarizing or hyperpolarizing phases of the oscillation and the extracellularly recorded field potentials. This raises the critical issue of the relation between the activity of one cell and the surrounding ones.

While recording a neuron (e.g., the area 7 cell in Fig. 3*A*), we were able to pick up with a different microelectrode the field potential in the adjacent area 5 (Fig. 3*A*), just before impaling a neuron in the track within area 5 (Fig. 3*B*). In this way, keeping the same reference (cell in area 7) before and after impaling area 5 cell, during the same EEG state, we obtained evidence about the relation of the impaled cell with its neighbors. During the initial period, before the impalement, the bursting area 7 cell oscillated synchronously with the focal waves from area 5 at a frequency of ~0.7 Hz. After impalement, the synchrony between extracellular spikes in area 7 and intracellular events in area 5 was preserved. The STAs in Fig. 3*C* were obtained by using as reference the first spike of an oscillatory cycle in area 7 neuron and show the tight synchrony between waves of area 5 (before and after impalement), area 7, and EEG. Here again the depolarizing events in the intracellular trace correspond to depth-negative field potentials of area 5 and 7 and to surface-positive deflections of EEG. Comparing the intracellular STA with the focal STA before impalement shows that the duration of the excitatory postsynaptic potential (EPSP) is shorter than that of the negative field potential,

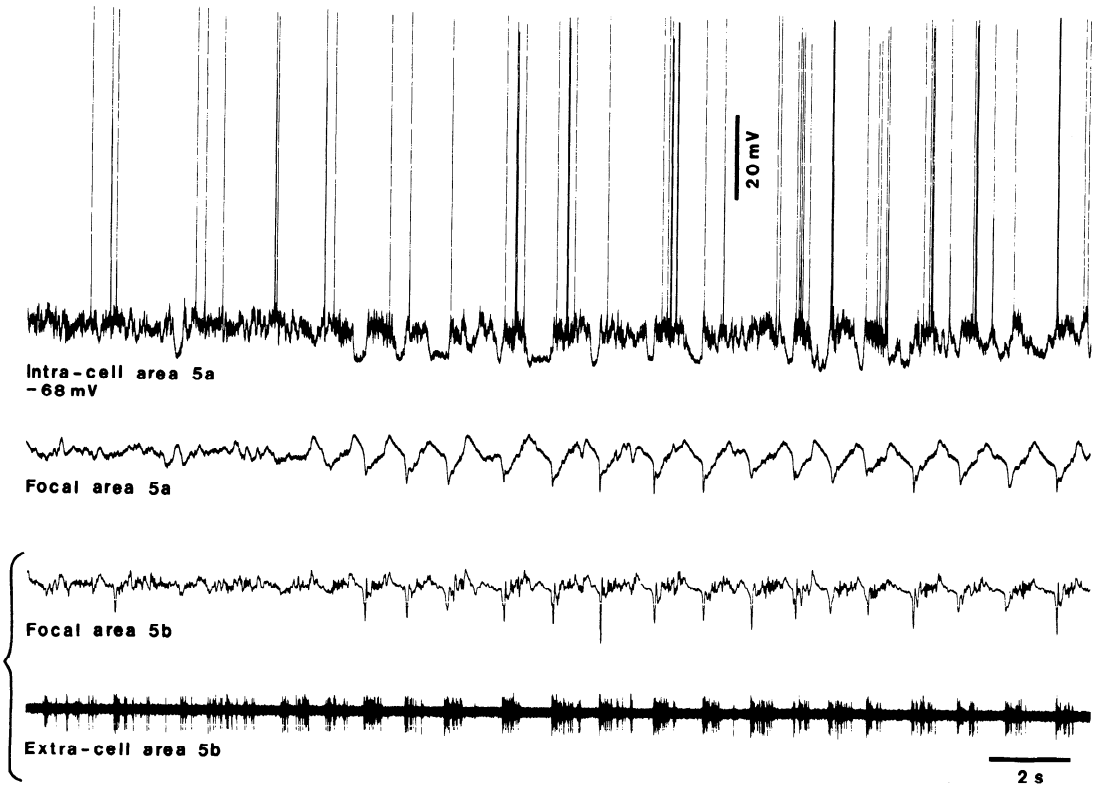

FIG. 1. Relations between focal (field) potentials, extracellular discharges, and intracellular activity in closely located cortical neurons. Simultaneous recordings from 3 foci of anterior suprasylvian areas 5a and 5b [for recording sites see brain scheme in Fig. 5 of the present paper as well as Fig. 37 in Hassler and Muhs-Clement (1964)]. The appearance of high-amplitude, rhythmic field potentials was accompanied by increased incidence of hyperpolarizations and rhythmic spike trains. In this and following figures, the polarity of field potentials and electroencephalographic (EEG) recordings is the same as for intracellular recordings (positivity up).

suggesting that several depolarizing waves from different units may build up the focal negativity.

Therefore the correlational analysis of field potentials may be used as a complementary tool to assess neuronal synchrony. The peak of the cross-correlation provides the time relation between the activities of two foci. In the case depicted in Fig. 4*A*, each of two microelectrodes, at 1 mm apart within area 5, recorded two neurons. All four cells were rhythmic at 0.6 Hz (2 autocorrelograms, 3 cross-correlograms, and 1 cross-correlation between field potentials within sites 1 and 2 are shown in Fig. 4*A*). The cross-correlogram between *cells 1a* and *2a* shows a central peak, probably due to a common input and/or a synchronized input arising largely from different sets of synchronized cells. Similar relations resulted from *cells 1a-2b* and *2a-2b* (not shown). The two cross-correlograms between *cells 1a-1b* and *1b-2a* had asymmetric central peaks with short time lags, in the order of 5–20 ms. The cross-correlation between the focal waves of the two foci displayed a well-defined peak.

The mean time lag between closely located cells (1–2 mm) in areas 5 and 7 was 12 ± 11.2 ms (range 0–140 ms) in a representative sample of cell groups (n = 70). In 70% of these cases (n = 49), the caudally located neurons preceded the rostral ones, and in 14% (n = 10) the contrary happened, whereas in the remaining 11 cases (16%) presumably common input patterns were observed (Fig. 4*B*). The mean correlation mark was 3.47 ± 0.72. The mean coherence mark was 2.02 ± 1.66.

In a few cases (n = 7), among simultaneous extracellular recordings, one neuron discharged high-frequency (>600 Hz) bursts of thin spikes (Fig. 5, *inset* from area 5b cell). These cells were tentatively regarded as local-circuit interneurons (McCormick et al. 1985; Steriade 1978). The spontaneous activity of the three neurons from areas 5a, 5b, and 7 showed a synchronous oscillatory pattern at ~0.5 Hz (Fig. 5). As in the great majority of our cases, this group of cells discharged during the depth-negative field potentials. However, the presumed interneuron discharged sometimes a first spike burst (*a* in rough data) at the onset of the depth-negative field potential; a second spike-burst (*b*) followed, by ~400 ms, falling on the rising slope of the depth-negative field potential. The two series of STAs (panel of averages, AVG in Fig. 5), calculated with the first spike in the interneuronal *burst a* (*left*) and *b* (*right*), demonstrate that the field potentials from areas 5b and 7 remained synchronized regardless of the firing of the fast-spiking cell. Note also that the shape of the STAs remained unchanged by shifting the reference from *burst a* to *burst b*. The cross-correlograms (Fig. 5, *bottom*) between the cell from area 5b and the other two neurons show high central peaks, equally distributed around 0 time lag.

Figure 6 shows simultaneous recordings from areas 5 and 7, accompanied by thalamic neurons from a related nucleus. Generally (58% of cases), thalamocortical and cortical cells oscillated synchronously at the slow frequency. In the group depicted in Fig. 6, the intracellularly recorded cell in area 7,

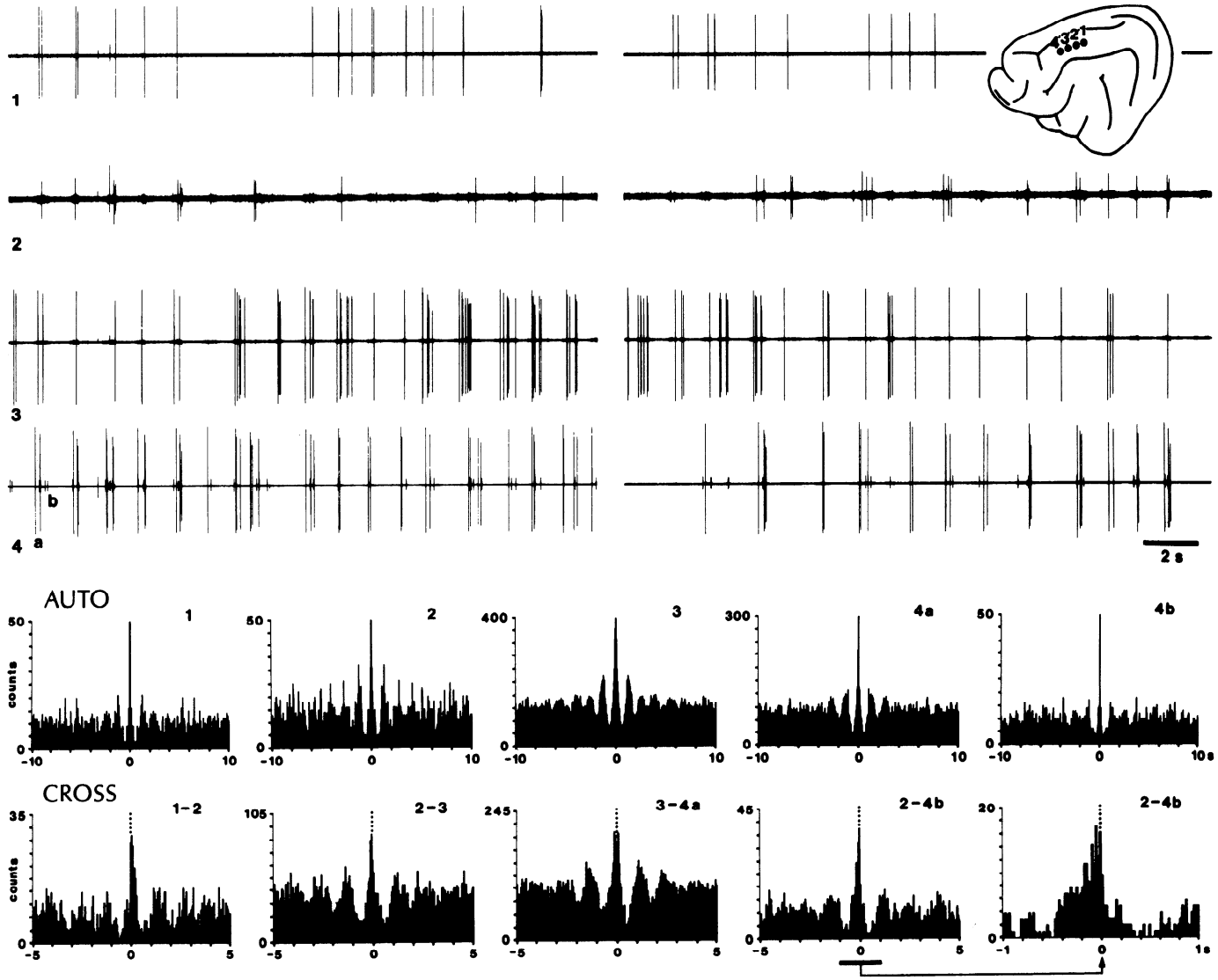

FIG. 2. Synchronization of slow oscillation in neurons recorded from 4 foci of cortical areas 5 and 7. In this and similar figures, brain scheme indicates the recording sites. Autocorrelograms of 5 cells demonstrate oscillation at ~0.7–0.8 Hz. Peaks in cross-correlograms (only 4 of 10 are depicted) show strong synchrony. The central peak from *cross-correlogram 2–4b* is expanded to show that discharges of *cell 2* preceded those of *cell 4b*.

the extracellularly recorded cell in area 5, and one of the centrolateral (CL) cells (small spike) discharged synchronously (see also *B*, were 7 sweeps were aligned on the depth-negative peak of the EEG wave and superimposed). The other CL neuron (large spike) fired ~220 ms later. The aspect of the thalamic field potentials (*B, bottom trace*) suggests that the recording electrode was juxtacellular to large-spike neuron, because spikes were associated with a focal positive deflection (probably the extracellular reflection of low-threshold spikes), whereas the discharges of small-spike cell were associated with a focal negativity. One of the sweeps from the thalamic recording are expanded in the *inset* (Fig. 6*B*) to show high-frequency bursts (250 Hz) in the two neurons.

Synchrony among cortical neurons from different areas of the visual system

The next series of data deal with multisite recordings from different cortical areas (17, 18, 19, and 21) and related thalamic nuclei (LG, lateral geniculate; PG, perigeniculate) of the visual system.

Simultaneous recordings in two association areas (18/19 and 21) of the visual cortex showed an average time lag of 27.6 ± 36 ms (range 5–160 ms) and a correlation mark of 2.9 ($n = 31$). In 70% of the cases, firing in area 21 preceded that in areas 18/19.

Figure 7*A* depicts a couple of such neurons, where the cell in area 21 is shown before impaling (Fig. 7*A1*) together with the field potentials, and after impaling (intracellular record in Fig. 7*A2*). The underlined sequence is expanded above to disclose the bursting pattern of the cell. Discharges in both recordings displayed a synchronous oscillation at ~0.5 Hz. The other panel (Fig. 7*B*) shows that even though the distance between the recording sites was greater than that in areas 5 and 7 (see above), the membrane fluctuations of area 21 cell was correlated with the discharges of the area 18 neuron. The fast excitatory events crowning the

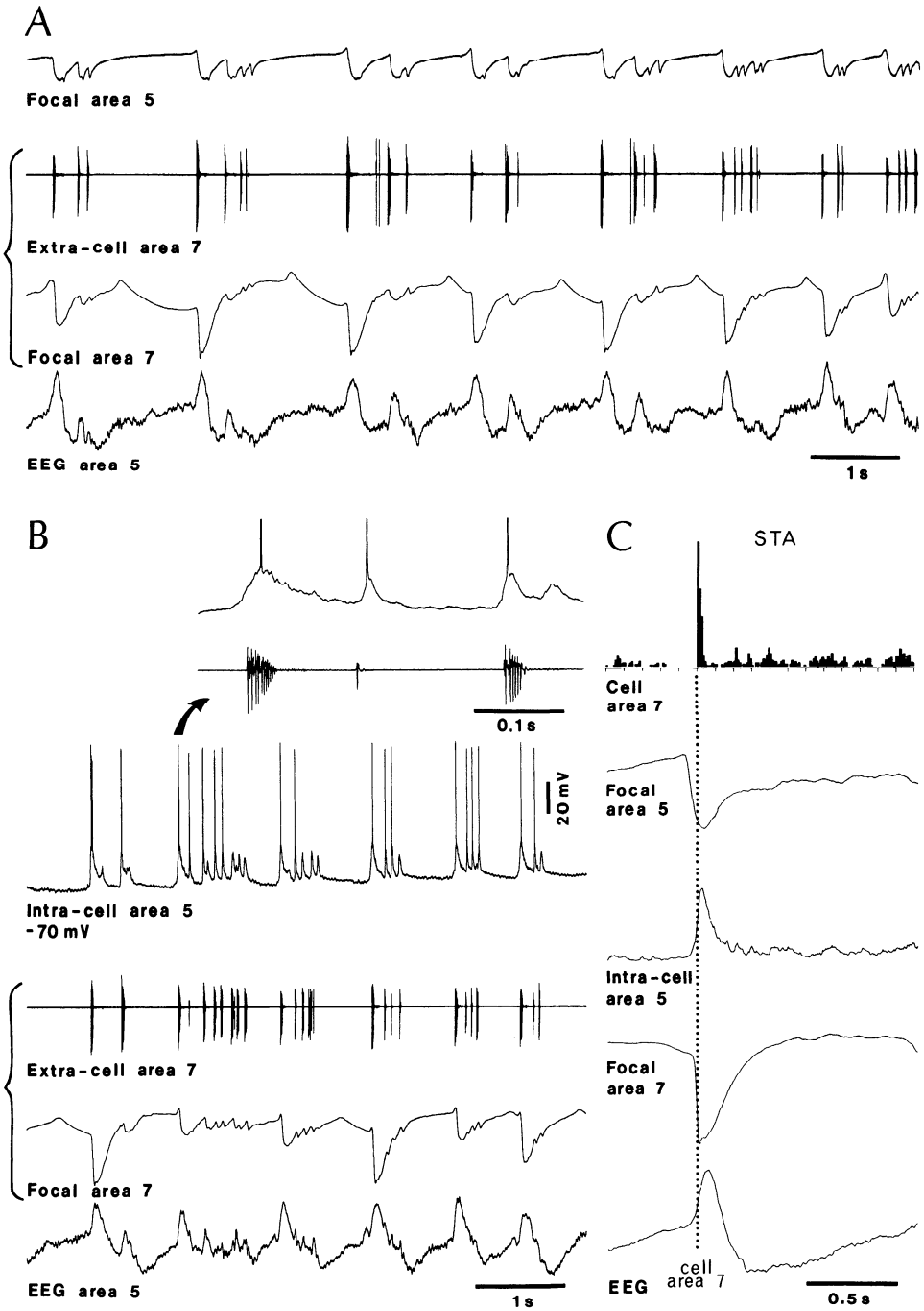

FIG. 3. Patterns of synchrony between extracellular discharges in area 7 and field potentials as well as intracellular activity in area 5. *A, top trace*: recording of focal waves through the same micropipette that eventually impaled the neuron showed in *top trace* in *B*. The extracellularly recorded area 7 neuron was a bursting cell (see *inset* indicated by arrow in *B;* intracellular action potentials truncated). *C*: 1st action potential in the 1st burst of area 7 cell, coincident with the beginning of a sharp depth negativity in area 7 (dotted line), was used for spike triggered averages (STAs) showing from top to bottom: the histogram of remaining spikes of area 7 cell (10-ms bins), focal waves in area 5, intracellular potentials (filtered at 30 Hz to eliminate action potentials), focal waves in area 7, and surface EEG.

depolarizing phase of the slow oscillation in the intracellular recording (see *inset* in Fig. 7*B*) occurred as a rule during the discharge of the other neuron, thus reflecting an increased excitation in the network.

The general synchronous oscillatory pattern could be seen throughout the visual cortices, including primary area 17 (Fig. 8). The simultaneous recordings of four neurons in areas 21, 18, and 17 (2 cells *a* and *b*) show a coherent oscillation at 0.85 Hz during which all neurons discharged synchronously and in phase with the onset of the focal depth negativity or surface positivity (see EEG area 18). Combined correlograms (black-filled, *bottom*) and correlations (above black-filled areas) are displayed to show the same oscillatory (AUTO) and time relation (CROSS) aspect of spike discharges and field potentials (Fig. 8). The peaks of the expanded three cross-correlations be-

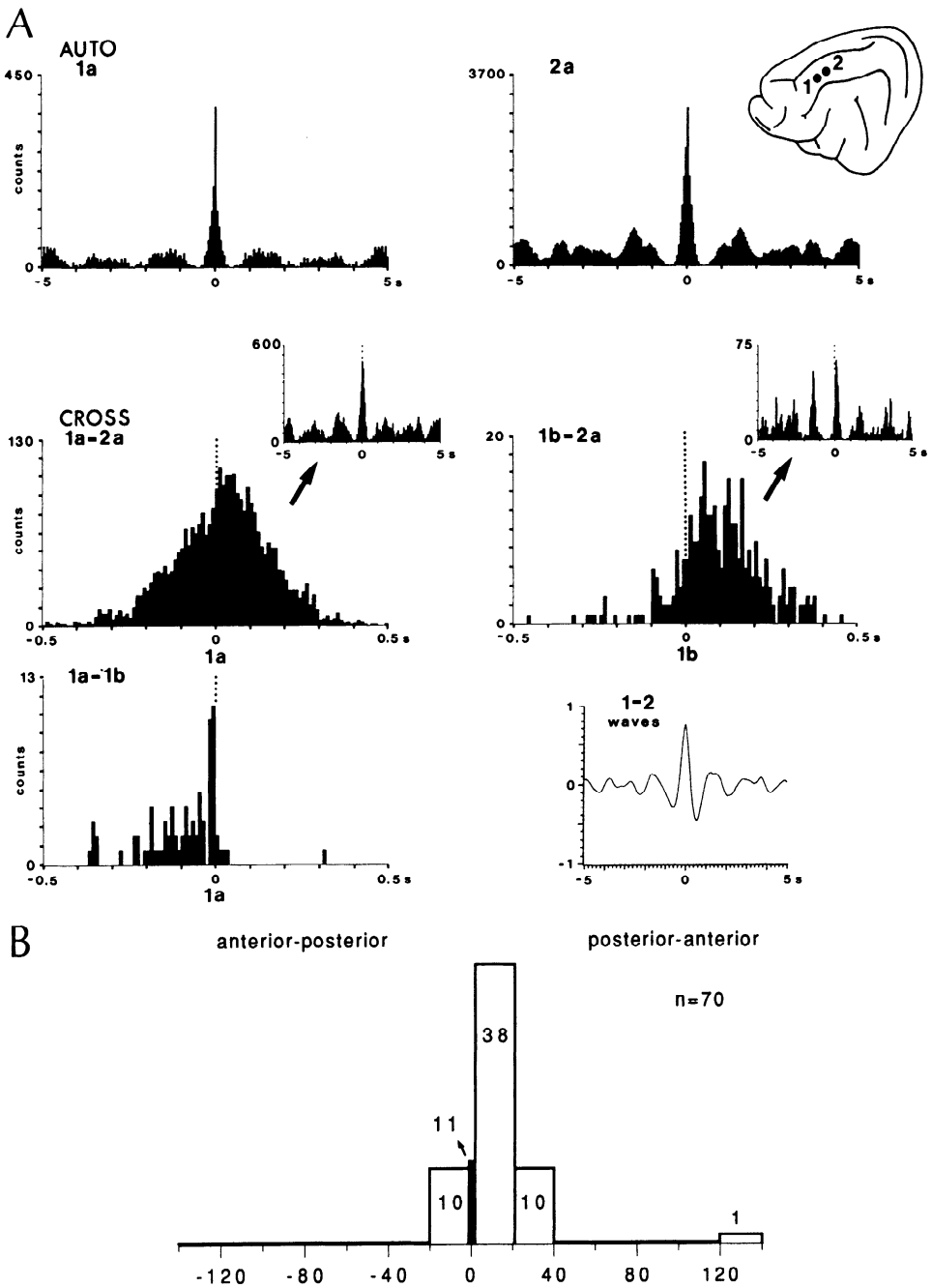

FIG. 4. *A*: synchrony in 2 foci of area 5, as shown by spike and field analyses. Each electrode picked up 2 neurons: *1a* and *1b* rostrally, and *2a* and *2b* caudally. All cells were rhythmic at 0.6 Hz (only 2 autocorrelograms are shown, AUTO). The temporal relation between their firing is shown in cross-correlograms (CROSS). *Top left cross-correlogram* (*1a-2a*) depicts a common input pattern. The other 2 cross-correlograms (*1b-2a, 1a-1b*) show relatively short time lags. *Insets* (marked by arrows in *1a-2a* and *1b-2a*) show the synchrony of the slow oscillation over a 5-s window. Field analysis shows a well-defined central peak in the cross-correlation (*1–2*). *B*: data from cross-correlograms in a sample of 70 cells recorded from anterior and posterior suprasylvian areas 5 and 7, showing the distribution of time lags between neuronal discharges (all time lags were calculated with the same 2-ms bin). Abscissa indicates time in 20-ms bins. Eleven neurons are represented at *time 0* (presumably common inputs). In other 10 neurons, discharges of anterior suprasylvian cells preceded those of posterior suprasylvian cells (time lags <20 ms). The remaining 49 neurons showed inverse relations, with a majority of posterior neurons (38) discharging before anterior ones with time lags <20 ms.

tween focal waves disclosed time lags of 10–15 ms (not shown).

This pattern of synchrony was found in 58% of cell groups including an area 17 recording (n = 26). The mean time lag separating discharges in areas 21 and 17 was 36.25 ± 47.8 ms (range 0–115 ms), whereas the time lag between discharges in areas 18 and 17 was 40 ± 73 ms (range 0–170 ms). In 19% of the cases, area 17 neurons oscillated at delta frequencies (Fig. 9), and in 23% of the cases they were arrhythmic and were therefore not synchronous with

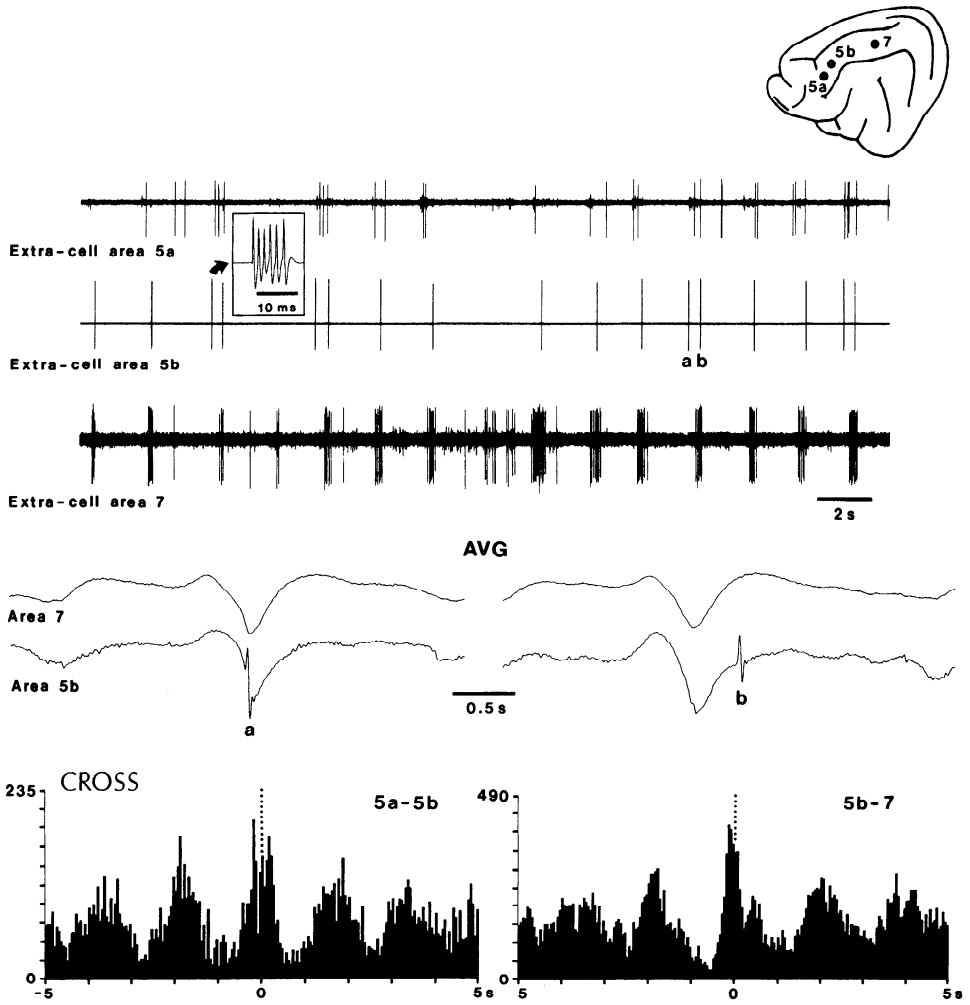

FIG. 5. Fast-spiking bursting cell, presumably interneuron, discharged synchronously with pyramidal cells. Cell in area 5b fired high-frequency (~600 Hz) action potentials of short duration (<0.7 ms; see *inset* marked by arrow). Bursts occurred during the negative phase of the field potential (see *B*) and synchronously with discharges of the other neurons. Note the double spike burst of bursting cell (*a* and *b*). When the neuron displayed just 1 burst, it was *b* one. Separate STAs (AVG, $n = 30$) for the 2 references (*a* and *b*) show the relation between focal waves of areas 5b and 7, and the distinct moments when the 2 spike bursts took place. Cross-correlograms between neurons from areas 5a, 5b, and 7 display a uniform disposition around 0 time lag.

slowly oscillating cells in association areas. The neurons in areas 21 and 18 illustrated in Fig. 9 oscillated, as shown by their respective autocorrelograms and by the FFTs of simultaneously recorded field potentials, at a frequency of ~0.65 Hz (other components <1 Hz are also disclosed by the FFTs). In area 17, another component appeared at 2.7 Hz (see arrow). This frequency also appears in the autocorrelogram of spike discharges. Although neurons in areas 21 and 18 kept the same relation pattern (CROSS 21–18) as described above, no synchrony was evident between cells in areas 21 and 17. The cross-correlations between areas 21–17 and 18–17 (above cross-correlograms) suggest a higher degree of synchrony than the respective cross-correlograms (Fig. 9).

The PG thalamic nucleus reflected the slow cortical oscillation in 75% ($n = 23$) of the multisite recordings. In Fig. 10, cross-correlograms between cortical and PG neurons show a synchronized oscillation at 0.7 Hz.

The coherence of the slow rhythm (<1 Hz) in visual cortical and thalamocortical cells from the LG nucleus was observed in 58% ($n = 14$) of the cases. This was due to either arrhythmic discharges in some cells (11%) or to rhythmic delta-oscillating thalamocortical units (31% of the cases; Fig. 11). In the latter case, the two cortical neurons (from areas 21 and 17) oscillated at ~0.6 Hz and were synchronous. No correlation could be disclosed between cortical and the two LG neurons. The latter displayed a clocklike delta oscillation at 2.7 Hz and were highly coherent.

Synchrony in distant recordings

The slow oscillation was found in many distant and functionally different neocortical areas (Steriade et al. 1993c). Our next approach was to record neurons belonging to more distant foci and, at the same time, to different sensory modalities. We kept one or several electrodes in areas 5 and 7 as a control for similar synchrony parameters and placed the other electrode(s) in the visual associational areas 21 and/or 18. Figure 12 shows that, during EEG-synchronized patterns, two neurons in area 21 (one of them recorded intracellu-

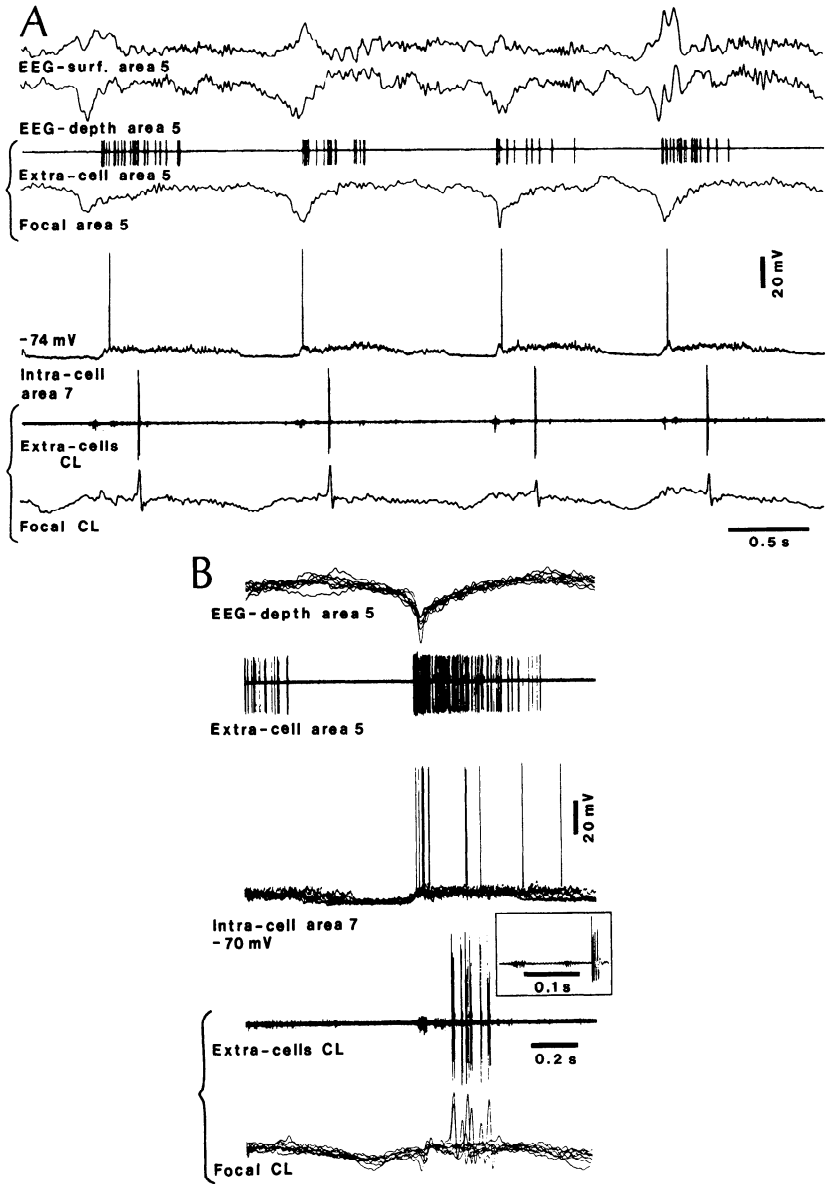

FIG. 6. Synchrony between neurons from cortical areas 5 and 7 and centrolateral intralaminar thalamic nucleus. *A*: 2 cortical neurons, extracellularly in area 5 (together with field potentials) and intracellularly in area 7, and 2 CL thalamic cells, were simultaneously recorded with surface and depth EEG from ipsilateral area 5 (1 mm apart from area 5 cell). EEG shows surface depth inverted phases during the slow oscillation; the peak negativity in the depth EEG was associated with cellular excitation and was followed by oscillations in the frequency range of spindles (10–14 Hz) and faster frequencies (30–40 Hz). *B*: 7 superimposed sweeps extracted from the same period of recording as shown in *A* and aligned on the negative peak of the depth EEG from area 5. Note short time lags between cortical neurons and small-spike CL neuron, whereas the large-spike CL neuron discharged only after ~0.2 s.

larly), two neurons in area 7, and one in area 5 oscillated synchronously at ~0.7 Hz. The onset of the spike trains was reliably preceded by sharp, high-amplitude negative focal waves, and hyperpolarizations in the intracellular trace correspond to silenced firing in the other neurons. As soon as the amplitude of the focal waves diminished and faster events replaced the slow waves, the synchronization was disturbed, and the intracellular neuron lacked the long-lasting hyperpolarizations that shaped the slow oscillation. As an argument for the use of field potentials as a reliable support for synchrony analysis, note the matching of the focal waves of the extracellularly recorded neuron in area 21 with the intracellular membrane potential fluctuations (Fig. 12*B*, *).

The widest spatial extent of our recordings covered simultaneously the motor and visual cortices (Fig. 13). Coherence was present between distantly located foci. Both spike and field analyses point to longer time lags as compared with those from close recordings (140 ms in Fig. 13*B*), with a mean of 124 ± 86.8 ms (range 20–260 ms).

DISCUSSION

We demonstrated that neurons recorded from closely or distantly located foci in association, visual, and motor cortical areas tend to discharge synchronously during the slow (<1 Hz) oscillation. To obtain stable recordings from multiple sites, including impalements of cortical cells, the slow rhythm was investigated under ketamine and xylazine anesthesia. To what extent was the rhythmic activity and its synchronization dependent on the properties of the present anesthetics? As to the rhythmic activity, similar slow (<1 Hz) oscillatory patterns were also observed in previous intracellular studies conducted under urethan anesthesia, in undrugged brain stem–transected animals, and at the EEG level in naturally sleeping cats and humans (Steriade et al. 1993c,d). Ketamine administration in urethan-anesthetized animals increases the frequency of slow oscillation, from ~0.3 Hz to ~0.6–0.9 Hz, because of the reduction in the duration of the depolarizing phase of the oscillation (Steriade

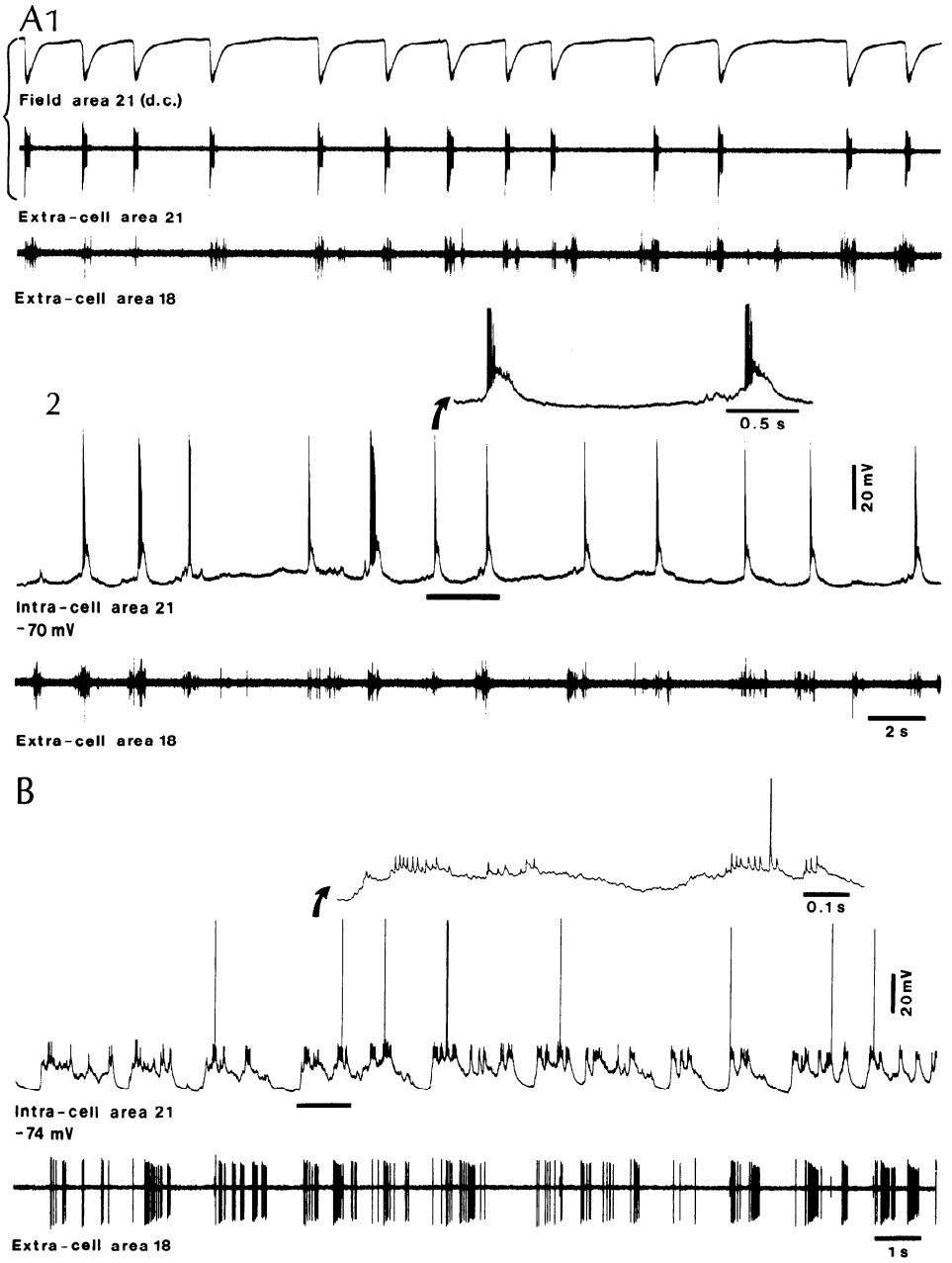

FIG. 7. Simultaneous recordings from visual association areas 21 and 18. *A1*: extracellular recordings from area 21 (field potential and unit discharges, before impaling this neuron; see *A2*) and area 18. *A2*: same couple after impaling area 21 cell. Epoch marked by horizontal bar is expanded above (arrow; spikes truncated) to show the bursting feature of neuron. *B*: another neuronal couple from areas 21 and 18, displaying a composite pattern of slow (~0.45 Hz) and delta (~4 Hz) oscillations. Epoch marked by horizontal bar is expanded above (arrow; spike truncated). Note synchrony between discharges in area 18 cell and intracellular membrane fluctuations.

et al. 1993c). This phase probably includes components mediated by *N*-methyl-D-aspartate (NMDA) receptors that are blocked by ketamine (MacDonald et al. 1991; Thomson 1986). Ketamine was administered during the state of waking and proved to significantly increase the amplitude and incidence of slow EEG waves during the state of sleep, thus placing this substance among the most effective pharmacological tools in inducing slow-wave sleep patterns (Feinberg and Campbell 1993). Even if ketamine anesthesia mimicks the electrical activity during slow-wave sleep, the degree of synchronization reported in the present paper probably exceeds that occurring during natural EEG-synchronized sleep. One likely possibility is that this increased synchronization is due to the combined use of xylazine, an $\alpha 2$ adrenoceptor agonist. Indeed, the effects mediated by $\alpha 2$ receptors are generally inhibitory and act by increasing a K^+ conductance in a variety of central structures (see Nicoll et al. 1990). The cyclic long-lasting hyperpolarizations, which are priming events toward the coherent activity of cortical neurons underlying the synchronization of slow oscillation (Contreras and Steriade 1995; Steriade et al. 1994b), are thought to be due, at least partially, to prolonged Ca^{2+}-

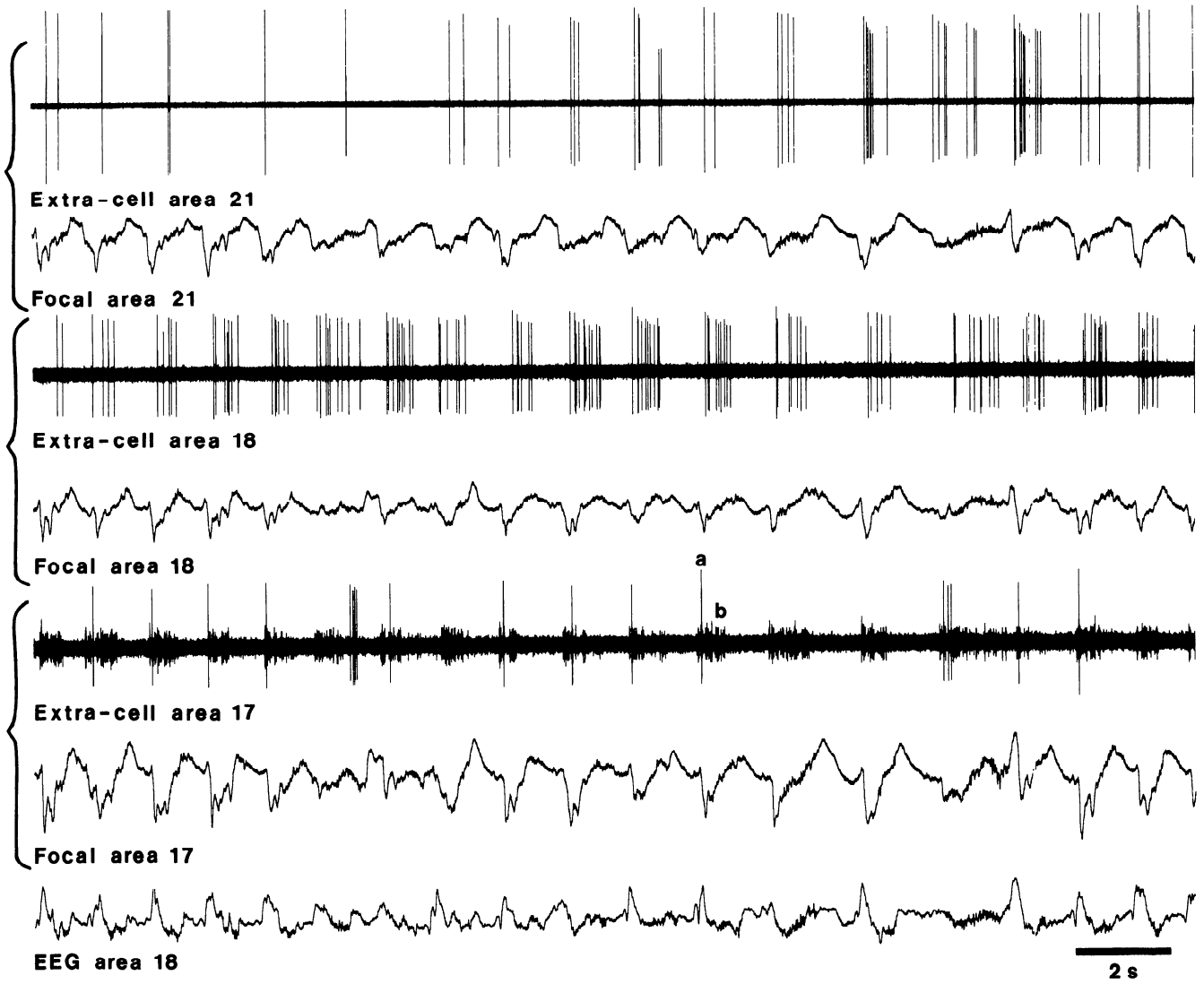
Extra-cell area 21
Focal area 21
Extra-cell area 18
Focal area 18
a
b
Extra-cell area 17
Focal area 17
EEG area 18
2 s

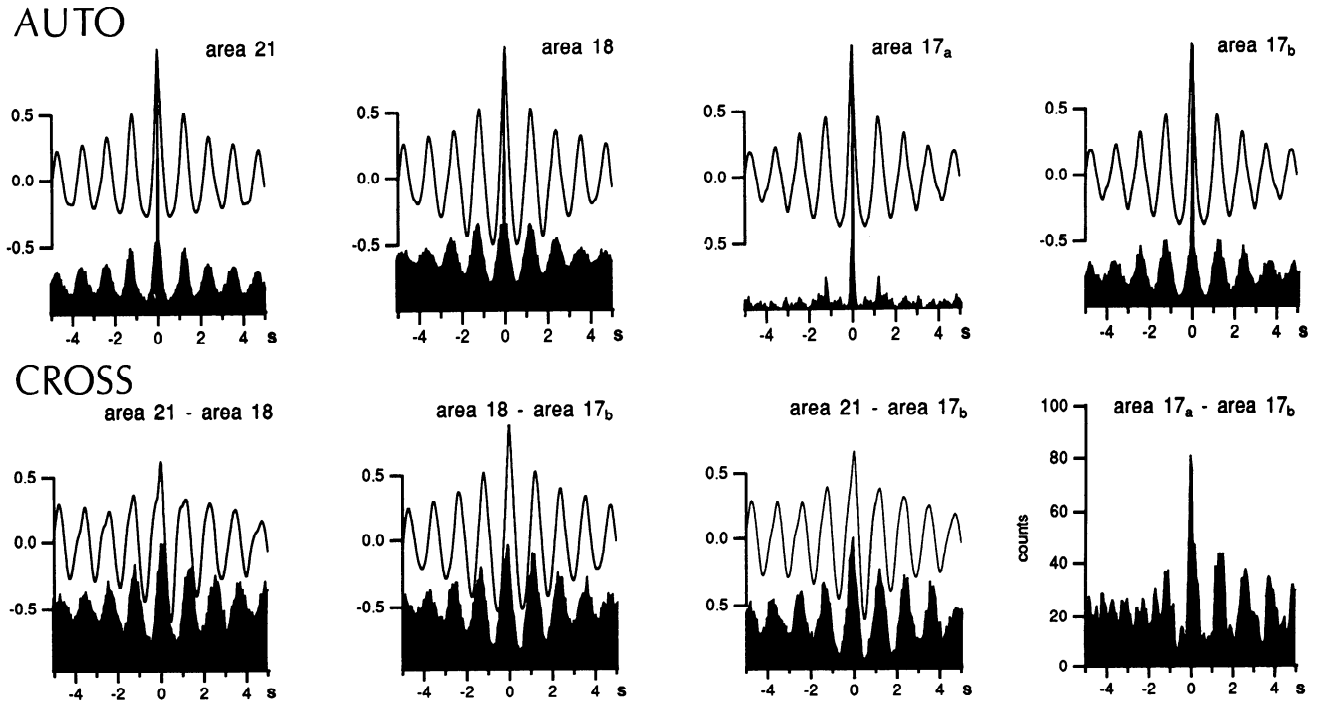
AUTO
area 21
area 18
area 17a
area 17b
CROSS
area 21 - area 18
area 18 - area 17b
area 21 - area 17b
area 17a - area 17b
counts

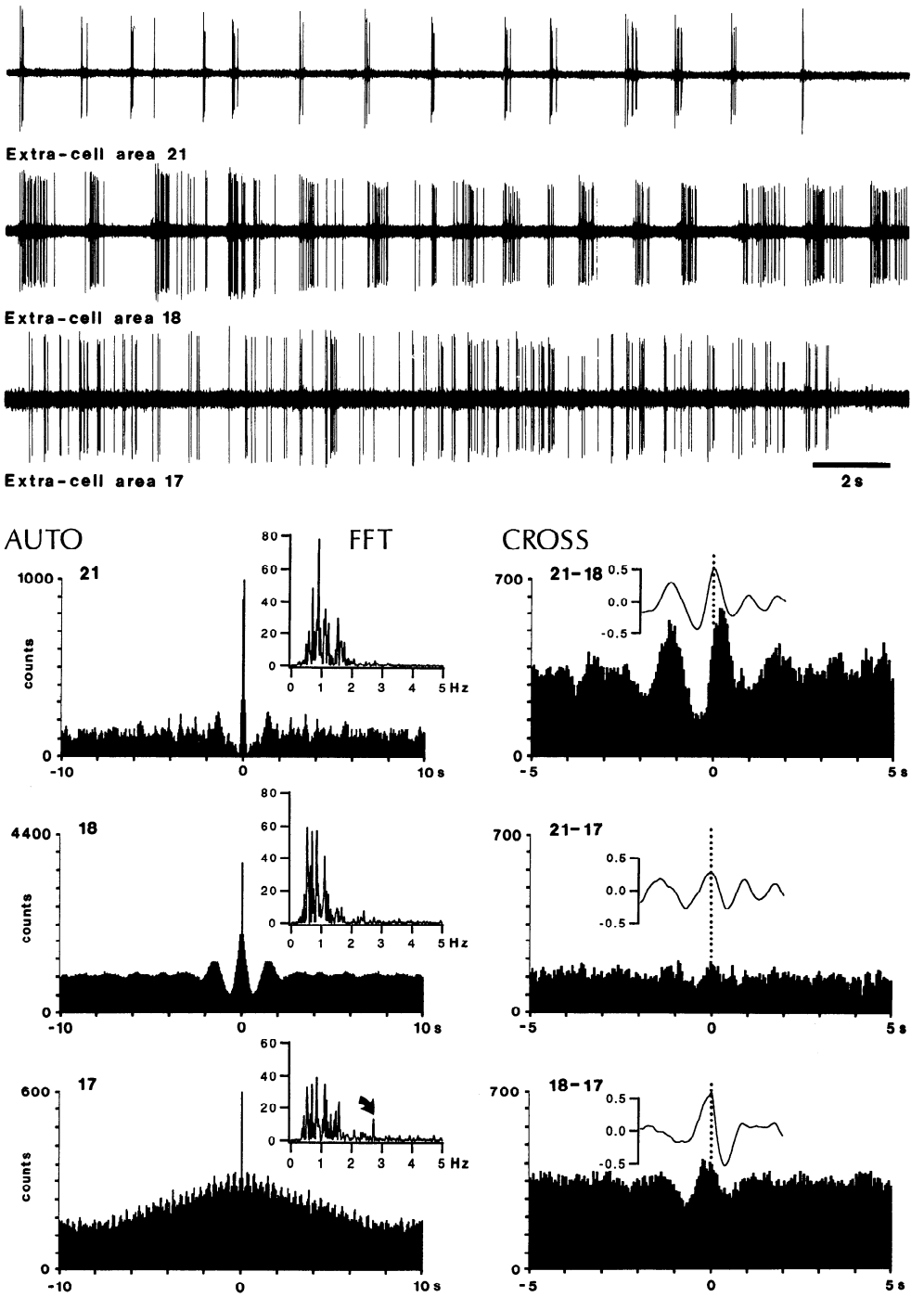

FIG. 9. Delta oscillation in primary area 17 cell, asynchronous with activities in visual association areas. Simultaneous recordings from areas 17, 18, and 21. *Top*: 2 cells from areas 21 and 18 oscillating at ~0.6 Hz, whereas area 17 cell displayed a faster rhythm, within the delta frequency range (2–3 Hz; see also fast Fourier transform (FFT) below). *Bottom*: autocorrelograms from the 3 cells. *Insets*: FFTs performed from the field potentials recorded through the same microelectrodes. Note autocorrelogram and FFT from area 17; arrow in FFT indicates a peak at 2.7 Hz. Cross-correlograms between the discharges of 3 cells (black-filled) and cross-correlations between field potentials (above).

FIG. 8. Synchrony between activities in primary and association visual cortices. *Top*: rough data displaying simultaneous recordings from areas 21, 18, and 17 (unit discharges and field potentials; 2 cells, *a* and *b*, recorded through the same microelectrode in area 17) as well as the surface EEG from area 18. The rhythmicity of the slow oscillation (~0.85 Hz) is demonstrated by autocorrelograms of spikes (black-filled). Cross-correlograms and cross-correlations show synchrony of the slow oscillation. Note also close time relation between the 2 neurons from area 17 (*a* and *b*) in spite of different discharge characteristics.

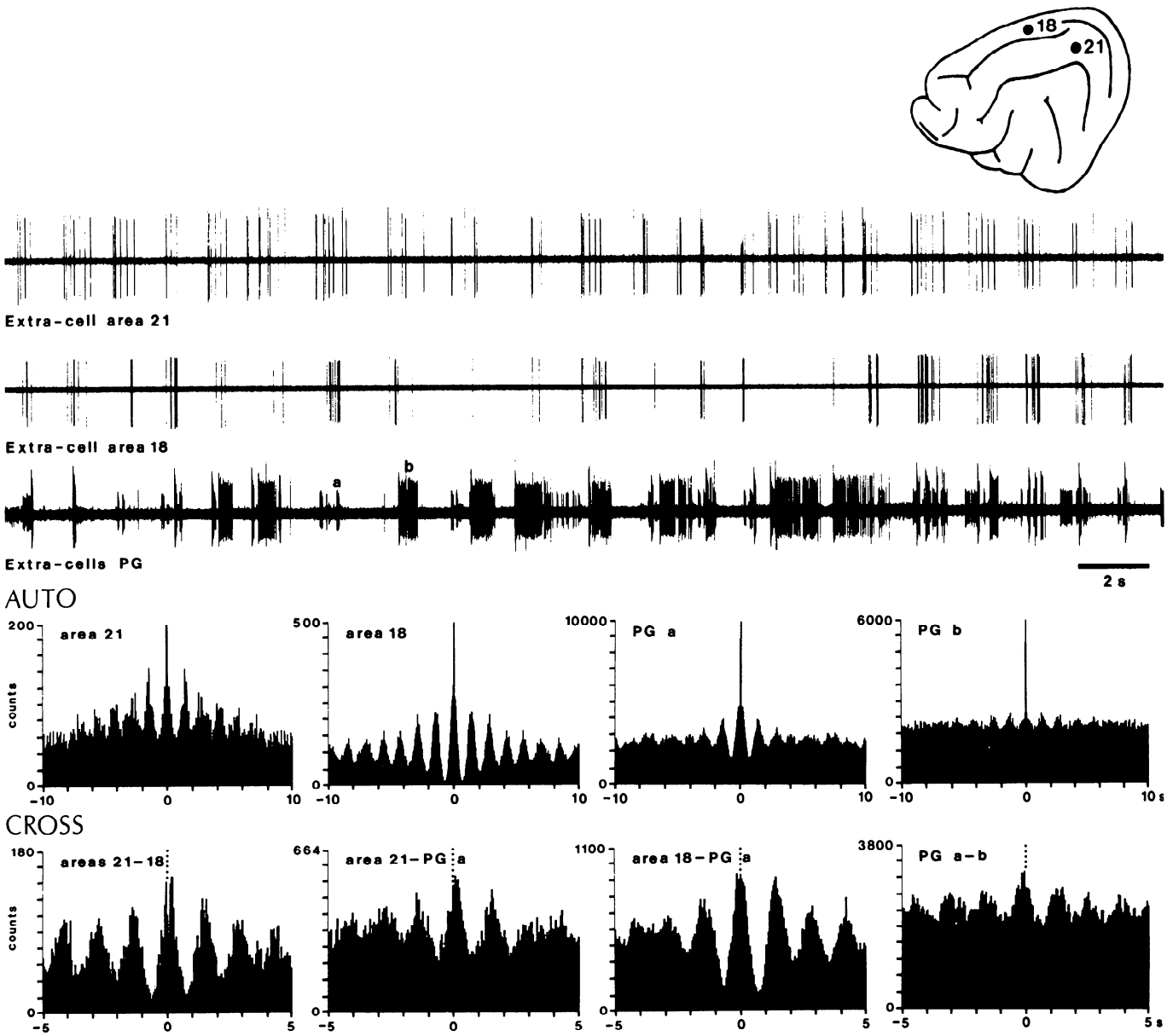

FIG. 10. Synchrony between cortical and reticular (perigeniculate (PG)) thalamic neurons. Triple extracellular recordings from cortical areas 21, 18, and the PG nucleus. Rhythmic slow (~0.7 Hz) oscillation (see autocorrelograms) and synchronous discharges between the recorded neurons (cross-correlograms). The degree of synchrony was quite low between neighboring PG cells (see CROSS *PGa-b*).

dependent K^+ currents (Steriade et al. 1993a). Substances that activate $\alpha 2$ receptors, such as xylazine or clonidine, increase the amplitude of long-lasting cyclic hyperpolarizations, and they also enhance the degree of EEG synchronization within the frequency range of slow rhythm (see Fig. 9 in Steriade et al. 1993a). Thus, although the pattern of the slow oscillation is qualitatively similar under ketamine and xylazine anesthesia (present experiments) and during natural slow-wave sleep (unpublished data), the degree of synchronization is probably enhanced under anesthesia.

Synchrony is a relative term. In the case of an oscillation with such a long period (>1 s), we considered two events as synchronous if the time lags were below one order of magnitude of the oscillation period. The mean time lag in cross-correlograms between closely located neurons (1–5 mm apart) in areas 5 and 7 was 12 ms. It was longer (from 27 to 40 ms) among neurons recorded at greater distances (5–10 mm) from different visual cortical areas or from visual and anterior suprasylvian association cortices, but could reach 125 ms when recordings were made from visual and motor cortices (~20–30 mm apart), although, in the latter case, relatively short time lags (~20 ms) were also detected. Thus, our data point to an average increase in time delays between cortical foci as a function of distance.

These time lags were derived from measures obtained by performing both spike and field analyses. In many instances, field potentials reflected the membrane potential fluctuations more faithfully than the extracellular action potentials (see Fig. 12*B*, *). The value of field potentials in assessing neuronal synchrony was also demonstrated in STAs showing

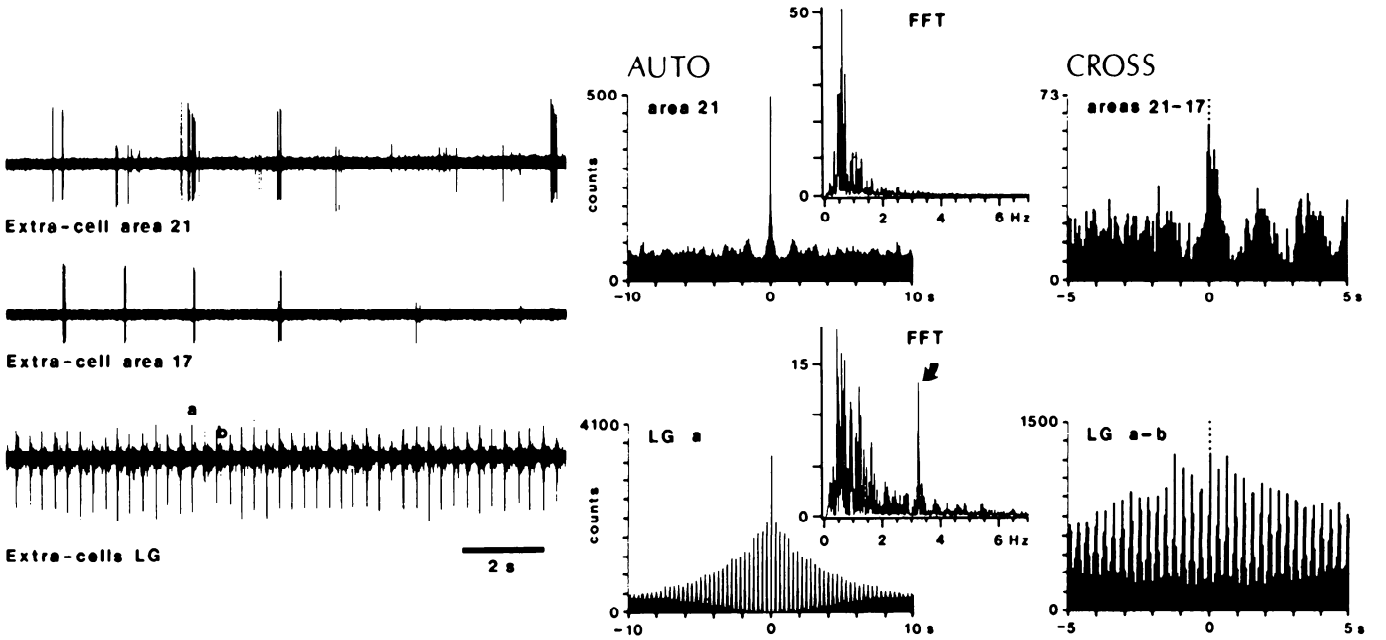

FIG. 11. Activities in visual cortical areas and lateral geniculate (LG) thalamic nucleus. Triple extracellular recordings from cortical areas 21, 17, and the LG nucleus. Although cortical neurons oscillated synchronously within the frequency of slow oscillation, ~0.6 Hz (see autocorrelogram of area 21, FFT of area 21, cross-correlograms areas 21–17), two LG cells (*a* and *b*) recorded through the same microelectrode oscillated synchronously at the delta frequency, as shown by autocorrelogram of *cell LGa* and the respective FFT of field potentials (arrow indicates a peak at 3.2 Hz) as well as *cross-correlograms LGa-b*.

similar time relations between the unit firing of the same cortical neuron when related to the field potential from an adjacent area and, immediately thereafter, to membrane fluctuations after impaling the neuron (Fig. 3, *A* and *B*).

Although some nonsynaptic factors may be decisive in the genesis of this generalized slow oscillation (see below), the consistent and relatively short time lags between different areas suggest that the intracortical synaptic circuitry is implicated in the propagation of slow oscillatory activity. In the cat association suprasylvian gyrus, where a major part of present experiments were conducted, the intrinsic circuitry probably accounts for >70% of the synapses (Grüner et al. 1974). Other studies, performed on visual and sensorimotor cortices, used electron microscopic examination of Golgi-impregnated, retrogradely labeled, or intracellularly stained neurons, and showed that the sources of local connections are both stellate and pyramidal-shaped neurons (for reviews, see Gilbert 1983; Jones 1988; Somogyi and Cowey 1984; White 1989). The local axonal collaterals of pyramidal cells form asymmetric synapses with spines of pyramidal and stellate neurons as well as with dendritic shafts of aspiny or sparsely spiny stellate cells. The axons of pyramidal neurons give rise to horizontal projections spanning up to 8 mm in visual cortex, thus allowing communication between neurons having widely separated receptive fields (Gilbert and Wiesel 1983; Mason et al. 1991; McGuire et al. 1991; Gilbert 1992). Horizontal projections have also been observed in other sensory areas (Imig and Reale 1981; Jones et al. 1978; Winfield et al. 1981). In addition to short- and medium-range intracortical projections, a series of studies revealed long-range corticocortical projections linking distant areas belonging to functionally different sensory and motor modalities (for reviews, see Goldman-Rakic 1988; Reinoso-Suárez 1984).

The above data suggest that, besides the intracolumnar and close intercolumnar operations mediated by a few synapses, the slow oscillation may propagate through long-range connections as each cortical area is connected to many other fields through direct and/or indirect linkages. Relatively short time lags suggest propagation through oligo- or multisynaptic excitatory connections. Long time lags (>50 ms) probably involve inhibition-rebound sequences in the cortex or within corticothalamocortical loops. Local inhibitory neurons are activated through feed-forward and feedback pathways (Nuñez et al. 1993; Toyama et al. 1969; Winfield et al. 1981), and, in turn, they project to both pyramidal cells (Matsubara et al. 1987) and other inhibitory interneurons (Kisvárday et al. 1993) located in the same or neighboring columns. Whereas low-threshold rebound spikes are ubiquitous in the thalamus (see review by Steriade and Llinás 1988), postinhibitory spike bursts seem to be present in only ~10% of neocortical neurons investigated in vivo (Nuñez et al. 1993), probably because the low-threshold Ca^{2+} current can be fully expressed in cortical cells at exceedingly negative membrane potentials, −100 mV (Sayer et al. 1990). This explains the scarcity of high-frequency spike bursts in cortical pyramidal cells during EEG-synchronized sleep (Evarts 1964; Steriade et al. 1974), as compared with those in thalamic cells where such bursts are a characteristic feature of resting sleep (see Steriade et al. 1990). Nonetheless, the propensity of cortical neurons to discharge at the very onset of the depolarizing phase, immediately after prolonged periods of hyperpolarizations, as consistently seen during the slow oscillation (see Figs. 7 and 8 in Steriade et al.

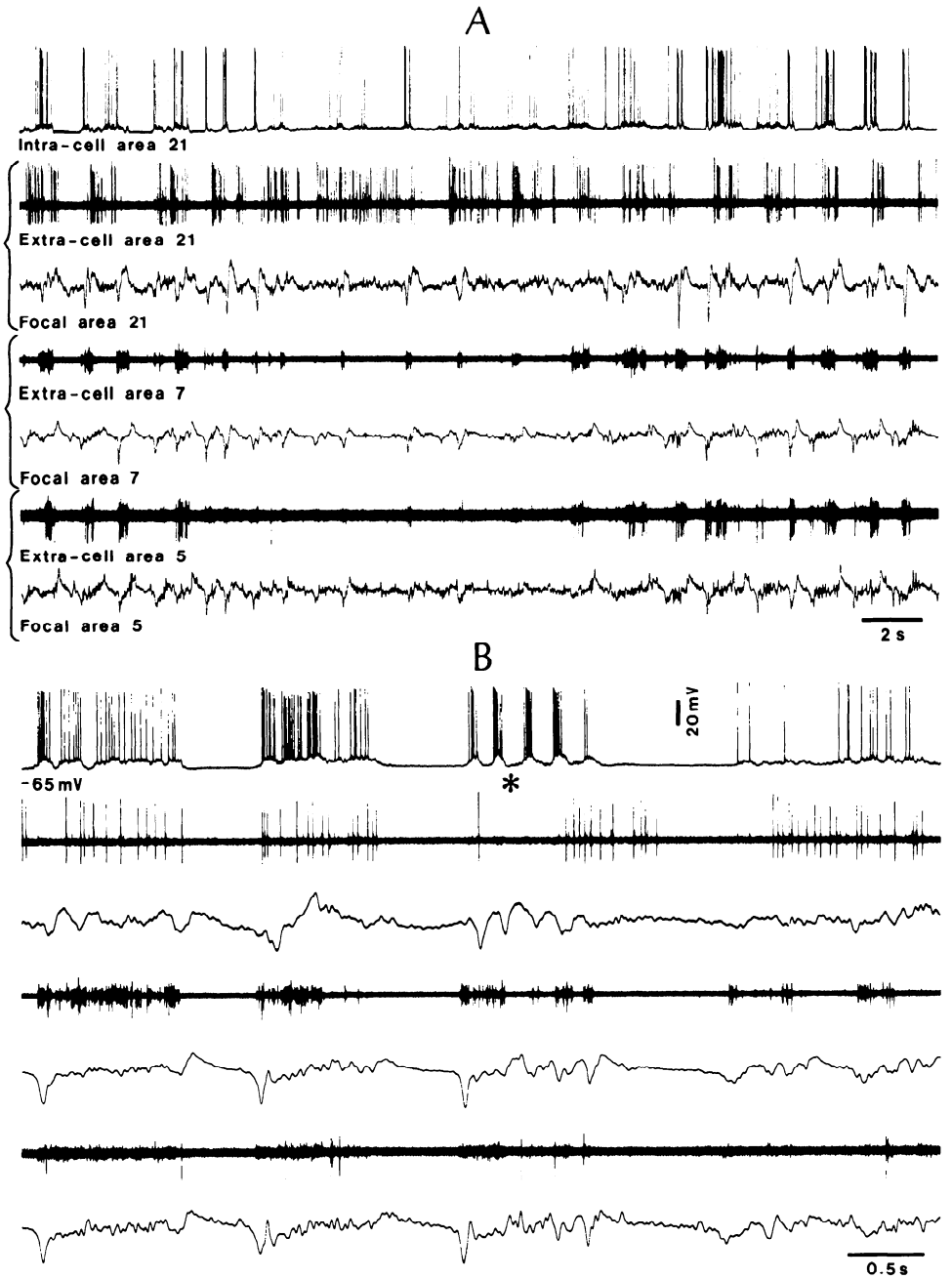

FIG. 12. Synchronization-desynchronization in distant recordings. Simultaneous recordings from areas 21 (intracellular and extracellular), 7, and 5 (extracellular spikes and field potentials). *A*: coherent oscillation in all 4 neurons was interrupted during a brief period of desynchronized activity (*middle*). *B*: same traces as in *A*. Oscillations recorded intracellularly better fit with focal waves than with extracellular spikes (asterisk).

1993c) (see also area 7 cell in the present Fig. 6*A*), suggests that postinhibitory rebound events, lacking the stereotypy of thalamic spike bursts and not yet fully understood, are decisive in starting the long-lasting depolarizing phase of the cortical slow oscillation. Besides, the rebound bursts of thalamocortical neurons occurring after the generalized inhibitory period of the slow oscillation, in phase with cortical discharges (Contreras and Steriade 1995) (also the present Fig. 6), may contribute to trigger the depolarizing phase of the oscillation. Thalamocortical afferents have access to cortical local circuits by driving both corticothalamic and aspiny multipolar cells engaged in a recurrent inhibitory circuit. Thus the excitation of aspiny neurons either by thalamocortical or corticothalamic input could cause them to inhibit corticothalamic cells (White and Keller 1987).

The two major types of pyramidal-shaped neurons, regular-spiking and intrinsically bursting cells, as described in vitro (Connors et al. 1982; McCormick et al. 1985) and in vivo (Nuñez et al. 1993), display the slow oscillation (Steriade et al. 1993c,d). The same oscillatory behavior was also observed in fast-spiking neurons and morphologically identified aspiny basket cells (Contreras and Steriade 1995). Vir-

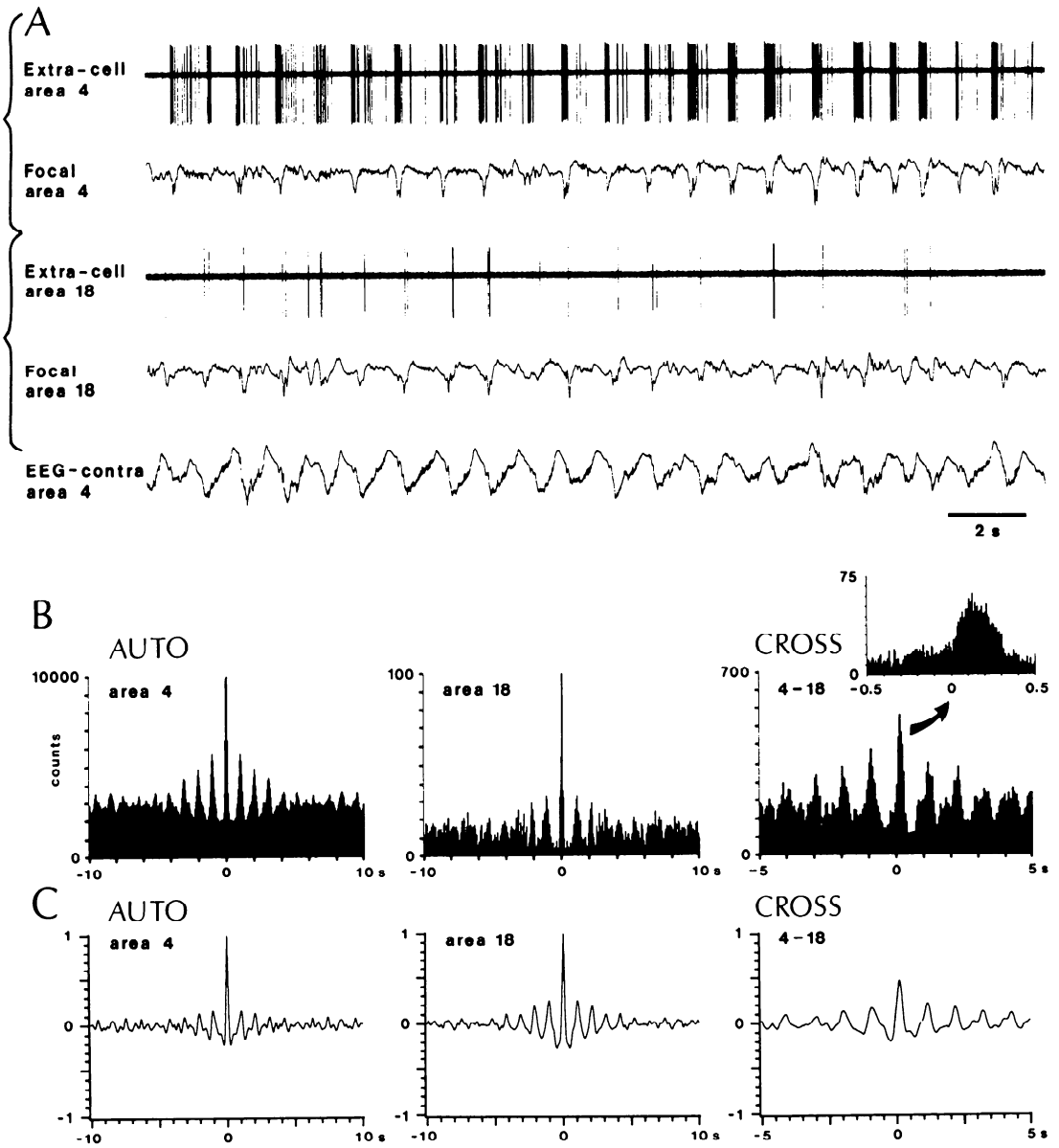

FIG. 13. Synchrony in distant recordings. *A*: 2 extracellular recordings (spikes and field potentials) from areas 4 and 18, together with contralateral EEG from area 4. *B*: autocorrelograms reveal rhythmic oscillation (~0.9 Hz) between neuronal discharges from areas 4 and 18, and cross-correlogram shows the coherence of the slow oscillation (*inset*, marked by arrow, shows a time lag of ~0.12–0.18 s between the 2 neurons). *C*: same analyses, but with focal waves, points to a time lag of 0.14 s between the oscillations in the 2 areas.

tually all aspiny cortical cells are regarded as GABAergic (Jones and Hendry 1986). Both pyramidal and aspiny local-circuit neurons display a similar phase relation to the EEG slow oscillation (Contreras and Steriade 1995). This accounts for sequences of repetitive inhibitory postsynaptic potentials (IPSPs) occurring in pyramidal neurons at depolarized levels and recurring at the frequency of the slow oscillation (see Fig. 6 in Steriade et al. 1993c). The fact that an overwhelming proportion of cortical cells, including inhibitory cells, discharge during the depolarizing phase of the slow oscillation (see Figs. 1, 3, 5, 7, and 8) suggests that the membrane conductance is significantly increased, thus diminishing the probability that single-axon EPSPs (Thomson et al. 1993; Thomson and West 1993) will elicit action potentials in target cells. Instead, the depolarizing envelope of the slow oscillation consists of compound PSPs triggering action potentials in a random way. This may explain the relative low incidence of short time lags in the present cross-correlograms.

The slow oscillation transcends the cortex and is transferred to the thalamus (Steriade et al. 1993b), striatum (Cowan and Wilson 1994), and upper brain stem core structures (Steriade et al. 1994a). Of all these distant structures, the thalamus is obviously the most likely candidate to influence, by feedback projections to the cortex, the slow oscillation. Whereas a great majority (75%) of PG reticular thalamic neurons reflected the slow cortical oscillation, a smaller percentage (58%) of LG thalamocortical neurons were coherent with slowly oscillating cortical neurons in the present experiments. Instead, a third of LG neurons dis-

played the intrinsically generated, clocklike delta oscillation (1–4 Hz), previously described in vitro (Leresche et al. 1991; McCormick and Pape 1990) and in vivo (Curró Dossi et al. 1992; Steriade et al. 1991). The spectacular synchrony of simultaneously recorded LG cells at the delta frequency (see cross-correlogram in Fig. 11) is in line with the demonstration that, in the LG nucleus, intrinsically delta-oscillating cells may be synaptically coupled through intranuclear axonal collaterals of thalamocortical neurons (Nuñez et al. 1992; Soltesz and Crunelli 1992). Besides the presence of the delta oscillation, thalamocortical cells fire fewer action potentials during the rhythmic depolarizations generated by the slow oscillation (Steriade et al. 1993b), probably because of the shunting of Na^+ spikes by inhibitory inputs from reticular thalamic (and possibly local thalamic) interneurons that are simultaneously driven during the cortically generated slow rhythm. Thus there is not yet definitive evidence whether or not the thalamus plays a significant role in synchronizing the slow cortical rhythm. The slow oscillation was present at the level of single cortical neurons after total lesions of appropriate thalamic nuclei (Steriade et al. 1993c), but further experiments with multisite recordings are needed to establish the role of thalamocortical neurons in intracortical synchrony. In this respect, emphasis should be placed on rostral intralaminar and ventromedial thalamic neurons that project widely on layer I of neocortex, where they contact the distal apical dendrites of deeply lying pyramidal cells (see Steriade et al. 1990). The horizontal layer I inputs evoke long-lasting EPSPs that may trigger active currents along the apical dendrites, involving both Na^+ and Ca^{2+}, thus amplifying the EPSP on its way to the soma (Cauller and Connors 1994). Together with the "backward" corticocortical projections traveling in layer I, these superficial thalamocortical projections may contribute significantly to the propagation of the slow oscillation.

The genesis and synchronization of slow oscillation are probably due to a combination of nonsynaptic and synaptic factors. The effects of ephaptic transmission were postulated to play a role in epileptic seizures in the hippocampus (Roper et al. 1993; Taylor and Dudek 1984a,b; Traub et al. 1985). However, at the level of neocortex, there is no substantial evidence that ephaptic effects may contribute to normally synchronized states. Two, metabolic and intrinsic, factors are considered here in the genesis of the slow oscillation. *1*) We have recently hypothesized (Steriade et al. 1994b) that the release of adenosine in the extracellular space, as a consequence of synchronous activity of many neurons during their prolonged depolarizations, may inhibit the cellular firing through an increase in a K^+ conductance. Such effects were described in the hippocampus (Haas and Greene 1988), thalamus (Pape 1992), and neocortex (McCormick and Williamson 1989), and the adenosine promoting effect of sleep was hypothesized to depend on an increase in K^+ conductance of arousing mesopontine cholinergic neurons (Rainnie et al. 1994). Adenosine can be slowly removed from the extracellular space, enabling neurons to fire, again releasing adenosine, and thus repeating the cycle. *2*) The role of a $g_{K(Ca)}$ in the genesis of prolonged hyperpolarizations during the slow oscillation was hypothesized in view of the blockage of this slow rhythm through a selective suppression of hyperpolarizing phases by stimulating mesopontine cholinergic nuclei (see Fig. 11*A* in Steriade et al. 1993a). It is known that acetylcholine suppresses $g_{K(Ca)}$ that produces long-lasting I_{AHPs} in neocortical cells (McCormick and Williamson 1989; Schwindt et al. 1988; Stafstrom et al. 1984).

We finally propose that the diminished firing rates in neurons of ascending diffuse modulatory systems from the very onset of sleep (see Steriade and McCarley 1990) lead to long-lasting hyperpolarizations in target cells, consequently leading to an avalanche disfacilitation in thalamic and cortical networks. The prolonged inhibitory periods favor the propensity to rebound spike bursts that constitute an efficient driving force for setting into action the cortical circuitry and developing sustained depolarizing phases in virtually all types of neurons. The possibility that metabolic factors, such as adenosine, would accumulate and induce cyclic hyperpolarizations sculpturing the slow oscillation should now be tested directly.

We thank P. Giguère and D. Drolet for technical assistance.

This work was supported by the Medical Research Council of Canada (Grant MT-3689). F. Amzica is a doctoral student.

Address reprint requests to M. Steriade.

Received 2 May 1994; accepted in final form 4 October 1994.

REFERENCES

ADRIAN, E. D. AND MATTHEWS, B. H. C. The interpretation of potential waves in the cortex. *J. Physiol. Lond.* 81: 440–471, 1934.

AERTSEN, A. M. H. J. AND GERSTEIN, G. L. Evaluation of neuronal connectivity: sensitivity of cross-correlation. *Brain Res.* 340: 341–354, 1985.

AMZICA, F. AND STERIADE, M. Synchronization of the slow (~0.3 Hz) oscillation in cortical networks. *Soc. Neurosci. Abstr.* 19: 1446, 1993.

BENDAT, J. S. AND PIERSOL, A. G. Engineering applications of correlation and spectral analysis. New York: Wiley, 1980.

CAULLER, L. J. AND CONNORS, B. W. Synaptic physiology of horizontal afferents to layer I in slices of rat SI neocortex. *J. Neurosci.* 14: 751–762, 1994.

CONNORS, B. W., GUTNICK, M. J., AND PRINCE, D. A. Electrophysiological properties of neocortical neurons in vitro. *J. Neurophysiol.* 48: 1302–1320, 1982.

CONTRERAS, D. AND STERIADE, M. Cellular basis of EEG slow rhythms: a study of dynamic corticothalamic relationships. *J. Neurosci.* 15: 604–622, 1995.

COWAN, R. L. AND WILSON, C. J. Spontaneous firing patterns and axonal projections of single corticostriatal neurons in the rat medial agranular cortex. *J. Neurophysiol.* 71: 17–32, 1994.

CURRÓ DOSSI, R., NUÑEZ, A., AND STERIADE, M. Electrophysiology of a slow (0.5–4 Hz) intrinsic oscillation of cat thalamocortical neurons in vivo. *J. Physiol. Lond.* 447: 215–234, 1992.

DICKSON, J. W. AND GERSTEIN, G. L. Interactions between neurons in auditory cortex of the cat. *J. Neurophysiol.* 37: 1239–1261, 1974.

ENGEL, A. K., KÖNIG, P., GRAY, C. M., AND SINGER, W. Stimulus-dependent neuronal oscillations in cat visual cortex: inter-columnar interaction as determined by cross-correlation analysis. *Eur. J. Neurosci.* 2: 588–606, 1992.

EVARTS, E. V. Temporal patterns of discharge of pyramidal tract neurons during sleep and waking in the monkey. *J. Neurophysiol.* 27: 152–171, 1964.

FEINBERG, I. AND CAMPBELL, I. G. Ketamine administration during waking increases delta EEG intensity in rat sleep. *Neuropsychopharmacology* 9: 41–48, 1993.

FETZ, E., TOYAMA, K., AND SMITH, W. Synaptic interactions between cortical neurons. In: *Cerebral Cortex,* edited by A. Peters. New York: Plenum, 1991, vol. 9, p. 1–47.

FROSTIG, R. D., GOTTLIEB, Y., VAADIA, E., AND ABELES, M. The effects of stimuli on the activity and functional connectivity of local neuronal groups in the cat auditory cortex. *Brain Res.* 272: 211–221, 1983.

GERSTEIN, G. L., PERKEL, D. H., AND SUBRAMANIAN, K. N. Identification of functionally related neural assemblies. *Brain Res.* 140: 43–62, 1978.

GILBERT, C. D. Microcircuitry in the visual cortex. *Annu. Rev. Neurosci.* 6: 217–247, 1983.

GILBERT, C. D. Horizontal integration and cortical dynamics. *Neuron* 9: 1–13, 1992.

GILBERT, C. D. AND WIESEL, T. N. Clustered intrinsic connections in cat visual cortex. *J. Neurosci.* 3: 1116–1133, 1983.

GOLDMAN-RAKIC, P. S. Changing concepts of cortical connectivity: parallel distributed cortical networks. In: *Neurobiology of Neocortex,* edited by P. Rakic and W. Singer. New York: Wiley-Interscience, 1988, p. 177–202.

GRÜNER, J. E., HIRSCH, J. C., AND SOTELO, C. Ultrastructural features of the isolated suprasylvian gyrus in the cat. *J. Comp. Neurol.* 154: 1–27, 1974.

GUREWITSCH, M. AND CHATSCHATURIAN, A. Zur Cytoarchitektonik der Grosshirnrinde der Feliden. *Z. Anat. Entwicklungsgesch.* 87: 100–138, 1928.

HAAS, H. L. AND GREENE, R. W. Endogenous adenosine inhibits hippocampal CA1 neurones: further evidence from extra- and intracellular recording. *Arch. Pharmacol.* 337: 561–565, 1988.

HASSLER, R. AND MUHS-CLEMENT, K. Architektonischer Aufbau des sensorimotorischen und parietalen Cortex der Katze. *J. Hirnforsch.* 6: 377–422, 1964.

IMIG, T. J. AND REALE, R. A. Ipsilateral corticocortical projections related to binaural columns in cat primary auditory cortex. *J. Comp. Neurol.* 203: 1–14, 1981.

JONES, E. G. What are local circuits? In: *Neurobiology of Neocortex,* edited by P. Rakic and W. Singer. New York: Wiley-Interscience, 1988, p. 137–152.

JONES, E. G., COULTER, J. D., AND HENDRY, S. H. C. Intracortical connectivity of architectonic fields in somatic sensory, motor and parietal cortex of monkeys. *J. Comp. Neurol.* 181: 291–348, 1978.

JONES, E. G. AND HENDRY, S. H. C. Colocalization of neuropeptides and GABA in the cerebral cortex. *Trends Neurosci.* 9: 71–76, 1986.

KISVÁRDAY, Z. F., BEAULIEU, C., AND EYSEL, U. T. Network of GABAergic large basket cells in cat visual cortex (area 18): implication for lateral disinhibition. *J. Comp. Neurol.* 327: 398–415, 1993.

KRÜGER, J. Simultaneous individual recordings from many cerebral neurons: techniques and results. *Rev. Physiol. Biochem. Pharmacol.* 98: 177–233, 1983.

LERESCHE, N., LIGHTOWLER, S., SOLTESZ, I., JASSIK-GERSCHENFELD, D., AND CRUNELLI, V. Low-frequency oscillatory activities intrinsic to rat and cat thalamocortical cells. *J. Physiol. Lond.* 441: 155–174, 1991.

MASON, A., NICOLL, A., AND STRATFORD, K. Synaptic transmission between individual pyramidal neurons of the rat visual cortex in vitro. *J. Neurosci.* 11: 72–84, 1991.

MACDONALD, J. F., BARTLETT, M. C., MODY, I., PAHAPILL, P., REYNOLDS, J. N., SALTER, M. W., SCHNEIDERMAN, J. H., AND PENNEFATHER, P. S. Actions of ketamine, phencyclidine and MK-801 on NMDA receptor currents in cultured mouse hippocampal neurones. *J. Physiol. Lond.* 432: 483–508, 1991.

MATSUBARA, J. A., CYNADER, M. S., AND SWINDALE, N. V. Anatomical properties and physiological correlates of the intrinsic connections in cat area 18. *J. Neurosci.* 7: 1428–1446, 1987.

MCCORMICK, D. A., CONNORS, B. W., LIGHTHALL, J. W., AND PRINCE, D. A. Comparative electrophysiology of pyramidal and sparsely spiny stellate neurons of the cortex. *J. Neurophysiol.* 54: 782–806, 1985.

MCCORMICK, D. A. AND PAPE, H. C. Properties of a hyperpolarization-activated cation current and its role in rhythmic oscillation in thalamic relay neurones. *J. Physiol. Lond.* 431: 291–318, 1990.

MCCORMICK, D. A. AND WILLIAMSON, A. Convergence and divergence of neurotransmitter action in human cerebral cortex. *Proc. Natl. Acad. Sci. USA* 86: 8098–8102, 1989.

MCGUIRE, B. A., GILBERT, C. D., RIVLIN, P. K., AND WIESEL, T. N. Targets of horizontal connections in macaque primary visual cortex. *J. Comp. Neurol.* 305: 370–392, 1991.

MOORE, G. P., PERKEL, D. H., AND SEGUNDO, J. P. Statistical analyis and functional interpretation of neuronal spike data. *Annu. Rev. Physiol.* 28: 493–522, 1966.

MURTHY, V. N. AND FETZ, E. E. Coherent 25- to 35-Hz oscillations in the sensorimotor cortex of awake behaving monkeys. *Proc. Natl. Acad. Sci. USA* 89: 5670–5674, 1992.

NICOLL, R. A., MALENKA, R. C., AND KAUER, J. A. Functional comparison of neurotransmitter receptor subtypes in mammalian central nervous system. *Physiol. Rev.* 70: 513–565, 1990.

NODA, H. AND ADEY, W. R. Firing of neuron pairs in cat association cortex during sleep and wakefulness. *J. Neurophysiol.* 23: 672–684, 1970.

NUÑEZ, A., AMZICA, F., AND STERIADE, M. Intrinsic and synaptically generated delta (1–4 Hz) rhythms in dorsal lateral geniculate neurons and their modulation by light-induced fast (30–70 Hz) events. *Neuroscience* 51: 269–284, 1992.

NUÑEZ, A., AMZICA, F., AND STERIADE, M. Electrophysiology of cat association cortical cells in vivo: intrinsic properties and synaptic responses. *J. Neurophysiol.* 70: 418–430, 1993.

PAPE, H. C. Adenosine promotes burst activity in guinea-pig geniculocortical neurones through two different ionic mechanisms. *J. Physiol. Lond.* 447: 729–733, 1992.

RAINNIE, D. G., GRUNZE, H. C. R., MCCARLEY, R. W., AND GREENE, R. W. Adenosine inhibition of mesopontine cholinergic neurons: implications for EEG arousal. *Science Wash. DC* 263: 689–692, 1994.

REINOSO-SUÁREZ, F. Connectional patterns in parietotemporooccipital association cortex of the feline cerebral cortex. In: *Cortical Integration,* edited by F. Reinoso-Suárez and C. Ajmone-Marsan. New York: Raven, 1984, p. 255–278.

ROPER, S. N., OBENAUS, A., AND DUDEK, F. E. Increased propensity for nonsynaptic epileptiform activity in immature rat hippocampus and dentate gyrus. *J. Neurophysiol.* 70: 857–862, 1993.

SAYER, R. J., SCHWINDT, P. C., AND CRILL, W. E. High- and low-threshold calcium currents in neurons acutely isolated from rat sensorimotor cortex. *Neurosci. Lett.* 120: 175–178, 1990.

SCHWINDT, P. C., SPAIN, W. J., FOEHRING, R. C., CHUBB, M. C., AND CRILL, W. E. Slow conductances in neurons from cat sensorimotor cortex in vitro and their role in slow excitability changes. *J. Neurophysiol.* 59: 450–467, 1988.

SINGER, W. Synchronization of cortical activity and its putative role in information processing and learning. *Annu. Rev. Physiol.* 55: 349–374, 1993.

SOLTESZ, I. AND CRUNELLI, V. A role for low-frequency, rhythmic synaptic potentials in the synchronization of cat thalamocortical neurons. *J. Physiol. Lond.* 457: 257–276, 1992.

SOMOGYI, P. AND COWEY, A. Double bouquet cells. In: *Cerebral Cortex. Cellular Components of the Cerebral Cortex,* edited by A. Peters and E. G. Jones. New York: Plenum, 1984, vol. 1, p. 337–360.

SMITH, W. S. AND FETZ, E. E. Effects of synchrony between corticomotoneuronal cells on post-spike facilitation of muscles and motor units. *Neurosci. Lett.* 96: 76–81, 1989.

STAFSTROM, C. E., SCHWINDT, P. C., FLATMAN, J. A., AND CRILL, W. E. Properties of subthreshold response and action potential recorded in layer V neurons from cat sensorimotor cortex in vitro. *J. Neurophysiol.* 52: 244–263, 1984.

STERIADE, M. Cortical long-axoned cells and putative interneurons during the sleep-waking cycle. *Behav. Brain Sci.* 3: 465–485, 1978.

STERIADE, M. AND AMZICA, F. Dynamic coupling among neocortical neurons during evoked and spontaneous spike-wave seizure activity. *J. Neurophysiol.* 72: 2051–2069, 1994.

STERIADE, M., AMZICA, F., AND CONTRERAS, D. Cortical and thalamic cellular correlates of electroencephalographic burst-suppression. *Electroencephalogr. Clin. Neurophysiol.* 90: 1–16, 1994a.

STERIADE, M., AMZICA, F., AND NUÑEZ, A. Cholinergic and noradrenergic modulation of the slow (~0.3 Hz) oscillation in neocortical cells. *J. Neurophysiol.* 70: 1385–1400, 1993a.

STERIADE, M., CONTRERAS, D., AND AMZICA, F. Synchronized sleep oscillations and their paroxysmal developments. *Trends Neurosci.* 17: 199–208, 1994b.

STERIADE, M., CONTRERAS, D., CURRÓ DOSSI, R., AND NUÑEZ, A. The slow (<1 Hz) oscillation in reticular thalamic and thalamocortical neurons: scenario of sleep rhythm generation in interacting thalamic and neocortical networks. *J. Neurosci.* 13: 3284–3299, 1993b.

STERIADE, M., CURRÓ DOSSI, R., AND NUÑEZ, A. Network modulation of a slow intrinsic oscillation of cat thalamocortical neurons: cortically induced synchronization and brainstem cholinergic suppression. *J. Neurosci.* 11: 3200–3217, 1991.

STERIADE, M., DESCHÊNES, M., AND OAKSON, G.Inhibitory processes and interneuronal apparatus in motor cortex during sleep and waking. I. Background firing and responsiveness of pyramidal tract neurons and interneurons. *J. Neurophysiol.* 37: 1065–1092, 1974.

STERIADE, M., JONES, E. G., AND LLINÁS, R. R. *Thalamic Oscillations and Signaling.* New York: Wiley, 1990.

STERIADE, M. AND LLINÁS, R. R. The functional states of the thalamus and the associated neuronal interplay. *Physiol. Rev.* 68: 649–742, 1988.

STERIADE, M. AND MCCARLEY, R. W. *Brainstem Control of Wakefulness and Sleep.* New York: Plenum, 1990.

STERIADE, M., NUÑEZ, A., AND AMZICA, F. A novel slow (<1 Hz) oscillation of neocortical neurons in vivo: depolarizing and hyperpolarizing components. *J. Neurosci.* 13: 3252–3265, 1993c.

STERIADE, M., NUÑEZ, A., AND AMZICA, F. Intracellular analysis of relations between the slow (<1 Hz) neocortical oscillation and other sleep rhythms of the electroencephalogram. *J. Neurosci.* 13: 3266–3283, 1993d.

TAYLOR, C. P. AND DUDEK, F. E. Excitation of hippocampal pyramidal cells by an electrical field. *J. Neurophysiol.* 52: 126–142, 1984a.

TAYLOR, C. P. AND DUDEK, F. E. Synchronization without active chemical synapses during hippocampal afterdischarges. *J. Neurophysiol.* 52: 143–155, 1984b.

THOMSON, A. M. A magnesium-sensitive postsynaptic potential in rat cerebral cortex resembles neuronal responses to *N*-methylaspartate. *J. Physiol. Lond.* 370: 531–549, 1986.

THOMSON, A. M., DEUCHARS, J., AND WEST, D. C. Large, deep layer pyramid-pyramid single axon EPSPs in slices of rat motor cortex display paired pulse and frequency-dependent depression, mediated presynaptically and self-facilitation, mediated postsynaptically. *J. Neurophysiol.* 70: 2354–2369, 1993.

THOMSON, A. M. AND WEST, D. C. Fluctuations in pyramid-pyramid excitatory postsynaptic potentials modified by presynaptic firing pattern and postsynaptic membrane potential using paired intracellular recordings in rat neocortex. *Neuroscience* 54: 329–346, 1993.

TOYAMA, T., MATSUNAMI, K., OHNO, T., AND TOKASHIKI, S. An intracellular study of neuronal organization in the visual cortex. *Brain Res.* 14: 518–520, 1969.

TRAUB, R. D., DUDEK, F. E., SNOW, R. W., AND KNOWLES, W. D. Computer simulations indicate that electrical field effects contribute to the shape of the epileptiform field potential. *Neuroscience* 15: 947–958, 1985.

WINFIELD, D. A., BROOKE, R. N. L., SLOPER, J. J., AND POWELL, T. P. S. A combined Golgi-electron microscopic study of the synapses made by the proximal axon and recurrent collaterals of a pyramidal cell in the somatic sensory cortex of the monkey. *Neuroscience* 6: 1217–1230, 1981.

WHITE, E. L. *Cortical Circuits: Synaptic Organization of the Cerebral Cortex. Structure, Function and Theory.* Boston: Birkhäuser, 1989.

WHITE, E. L. AND KELLER, A. Intrinsic circuitry involving the local axon collaterals of corticothalamic projection cells in mouse SmI cortex. *J. Comp. Neurol.* 262: 13–26, 1987.